Journal of Medicinal Chemistry

Article

pubs.acs.org/jmc

β-Sulfonamido Functionalized Aspartate Analogues as Excitatory Amino Acid Transporter Inhibitors: Distinct Subtype Selectivity Profiles Arising from Subtle Structural Differences

Jacob C. Hansen, Walden E. Bjørn-Yoshimoto, Niels Bisballe, Birgitte Nielsen, Anders A. Jensen, and Lennart Bunch*

Department of Drug Design and Pharmacology, Faculty of Health and Medical Sciences, University of Copenhagen, Universitetsparken 2, Copenhagen Ø 2100, Denmark

Supporting Information

ABSTRACT: In this study inspired by previous work on 3-substituted Asp analogues, we designed and synthesized a total of 32 β-sulfonamide Asp analogues and characterized their pharmacological properties at the excitatory amino acid transporter subtypes EAAT1, EAAT2, and EAAT3. In addition to several potent EAAT inhibitors displaying IC_{50} values ~1 μM at all three subtypes, this elaborate structure−activity relationship also identified analogues exhibiting distinct preferences or selectivities for specific transporter subtypes. Introduction of two fluorine atoms on the phenyl ring yielded analogue **4y** that displayed an IC_{50} of 0.8 μM at EAAT1 with a 14- and 9-fold preference over EAAT2 and EAAT3, respectively. Conversely, the *m*-CF_3-phenyl analogue **4r** was a potent selective EAAT2-inhibitor (IC_{50} = 2.8 μM) exhibiting 30- and 50-fold selectivity over EAAT1 and EAAT3, respectively. In conclusion, even small structural differences in these β-sulfonamide Asp analogues provide analogues with diverse EAAT subtype selectivity profiles.

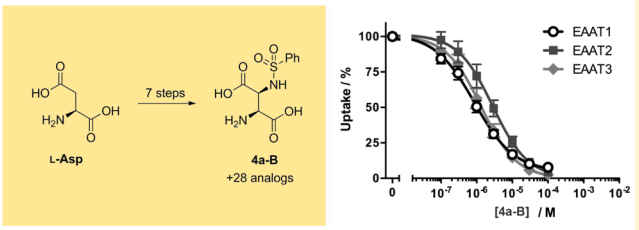

INTRODUCTION

(*S*)-Glutamate (Glu, Figure 1A) is the major excitatory neurotransmitter in the central nervous system (CNS), where it controls and regulates an immense number of different processes. Because of this abundance and the importance of glutamatergic neurotransmission for virtually all central functions, hyperactivity or hypoactivity in these systems are believed to be at the core of numerous cognitive, psychiatric, neurotoxic, and neurodegenerative disorders. Thus, the considerable therapeutic interest in glutamatergic targets is rooted in the possibility that these disorders as well as others not based in glutamatergic dysfunction potentially could be treated through this neurotransmitter system.[1−4]

The synaptic uptake of Glu following its release into the synaptic cleft is mediated by the five members of the excitatory amino acid transporter (EAAT) family, EAAT1−5.[5−10] These high-affinity Glu transporters are expressed in the plasma membranes of glia cells (predominantly EAAT1,2) and neurons (predominantly EAAT3−5). EAAT2 is the major EAAT subtype estimated to be responsible for >90% of total Glu uptake in the brain, with EAAT1 and EAAT3 also being abundantly distributed throughout the CNS. In contrast, EAAT4 and EAAT5 are almost exclusively expressed in cerebellar Purkinje cells and in the retina, respectively, and these subtypes also exhibit distinct transporter/channel properties compared to the other three EAATs and thus are believed to act predominantly as Cl^- channels.[5,6,8] The distinct regional and cellular distribution of the five EAAT subtypes in the CNS is likely to be important for their regulation of glutamatergic neurotransmission, just as selective modulation of the Glu uptake through different transporter subtypes may have different impact on glutamatergic neurotransmission, both when it comes to the characteristics and levels of the induced effects but also in terms of the CNS regions affected.

The potential in EAATs as therapeutic targets has so far not been explored to the extent as is the case in the Glu receptor fields,[11] and the limited selection of potent and truly subtype-selective EAAT modulators identified to date constitutes an obstacle to the delineation of the physiological roles and the therapeutic potential of each of the five transporters. Medicinal chemistry development in the EAAT field has mainly been based on the endogenous transporter substrates Glu and (*S*/*R*)-aspartate (Asp).[6] Several nonselective substrates and competitive nonsubstrate inhibitors of the transporters have emerged from these efforts, DL-*threo*-β-benzyloxyaspartate (TBOA)[12,13] being the prototypic nonselective EAAT inhibitor. Interestingly, EAAT2-selectivity has emerged from quite different modifications to the Glu and Asp structures, as EAAT2-selective inhibitors include the conformationally restricted Glu analogue dihydrokainic acid (DHK),[14,15] the 4-substituted Glu analogue (2*S*,4*R*)-2-amino-4-(3-(2,2-dipheny-

Received: July 18, 2016

DOI: 10.1021/acs.jmedchem.6b01066
J. Med. Chem. XXXX, XXX, XXX−XXX

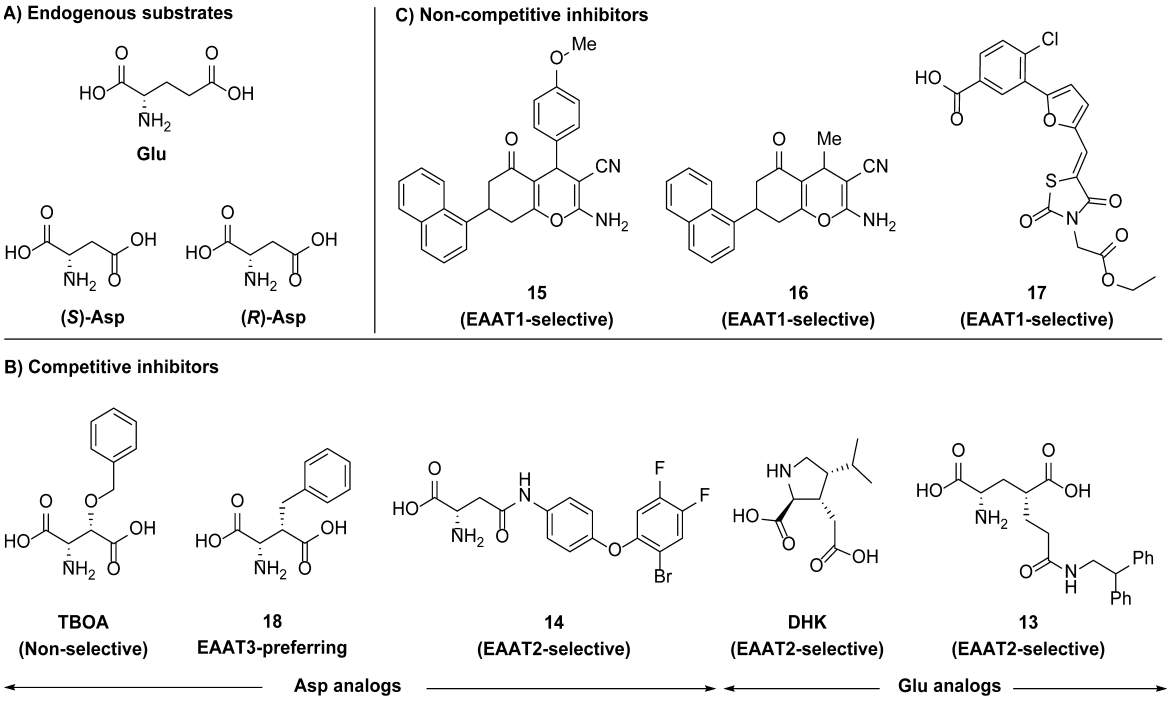

Figure 1. Chemical structures of: (A) Endogenous EAAT substrates Glu and Asp. (B) Competitive EAAT inhibitors TBOA,[12] **18**,[25] **14**,[17] DHK,[14,15] and **13**.[16] (C) Noncompetitive EAAT1 inhibitors **15**,[21] **16**,[22] and **17**.[24]

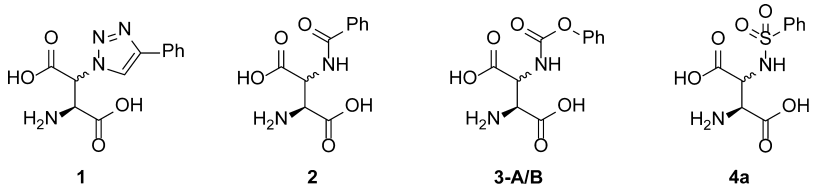

Figure 2. Chemical structures of rationally designed β-functionalized Asp analogues **1**, **2**, **3-A/B**, and **4a**.

lethylamino)-3-oxopropyl)pentanedioic acid (**13**),[16] and the functionalized asparagine analogue *N*-[4-(2-bromo-4,5-difluorophenoxy)phenyl]-L-asparagine (**14**, WAY-213613)[17] (Figure 1B). Although 4-methyl-Glu is a substrate of EAAT1 and a nonsubstrate inhibitor of EAAT2,3 and thus exhibits functional EAAT1-selectivity,[18,19] the only truly selective EAAT1 inhibitors reported to date are the noncompetitive inhibitors 2-amino-4-(4-methoxyphenyl)-7-(naphthalen-1-yl)-5-oxo-5,6,7,8-tetrahydro-4*H*-chromene-3-carbonitrile (**15**, UCPH-101),[20,21] 2-amino-4-(4-methyl)-7-(naphthalen-1-yl)-5-oxo-5,6,7,8-tetrahydro-4*H*-chromene-3-carbonitrile (**16**, UCPH-102),[22,23] and most recently (*Z*)-4-chloro-3-(5-((3-(2-ethoxy-2-oxoethyl)-2,4-dioxothiazolidin-5-ylidene)methyl)-furan-2-yl)benzoic acid (**17**)[24] (Figure 1C). Truly subtype-selective modulators of EAAT3−5 have yet to be discovered, but interestingly the β-substituted Asp analogue L-*threo*-β-benzylaspartate (**18**, L-β-BA)[25] has been reported to display a 10-fold preference as an inhibitor of EAAT3 over EAAT1,2.

Over the past decade, we have applied various approaches in our efforts to discover subtype-selective EAAT ligands.[6,16,19,21,26] In the present study, we were inspired by the previously reported work on 3-substituted Asp analogues as EAAT inhibitors, where the initial discovery of the nonselective EAAT substrate L-*threo*-β-hydroxyaspartic acid[15,27] has led to subsequent development of the nonselective EAAT inhibitor TBOA[12,13] and the more potent and EAAT1,2-preferring inhibitor TFB-TBOA[28,29] as well as to the EAAT3-preferring inhibitor **18**.[25] To explore the potential in the 3-substituted Asp analogue as a scaffold for EAAT ligands further, we have designed and synthesized a series of β-amino-Asp analogues and characterized their pharmacological properties at EAAT1−3. On the basis of this elaborate structure−activity relationship (SAR) study, we report that even small structural differences in the 3-substituents of these analogues give rise to dramatically different functional profiles at EAAT1−3.

RESULTS AND DISCUSSION

In view of the stereochemical match (*threo*)[30] and structural similarity of Asp analogues TBOA and **18**, we hypothesized that the functionality in the β-position of Asp plays a decisive role for the observed EAAT-selectivity profile and that this difference in pharmacology is likely to arise from differential spatial orientation of the aryl group in the substrate binding pocket of the EAAT. We therefore designed new series of β-amino-Asp analogues **1**−**4a** (Figure 2) to explore the orientation of the aryl group as well as its distance from the Asp scaffold on inhibitory activity.

Synthesis of 1, 2, 3-A/B, and 4a. The apparently important orientation of the phenyl ring in the Asp analogues **18** and TBOA urged us to reduce the degree of rotational freedom between the Asp backbone and the aromatic ring. To install this structural restriction, we opted for the incorporation

DOI: 10.1021/acs.jmedchem.6b01066
J. Med. Chem. XXXX, XXX, XXX−XXX

Scheme 1. Synthesis of β-Functionalized Asp Analogues 1, 2, 3-A/B, and 4a[a]

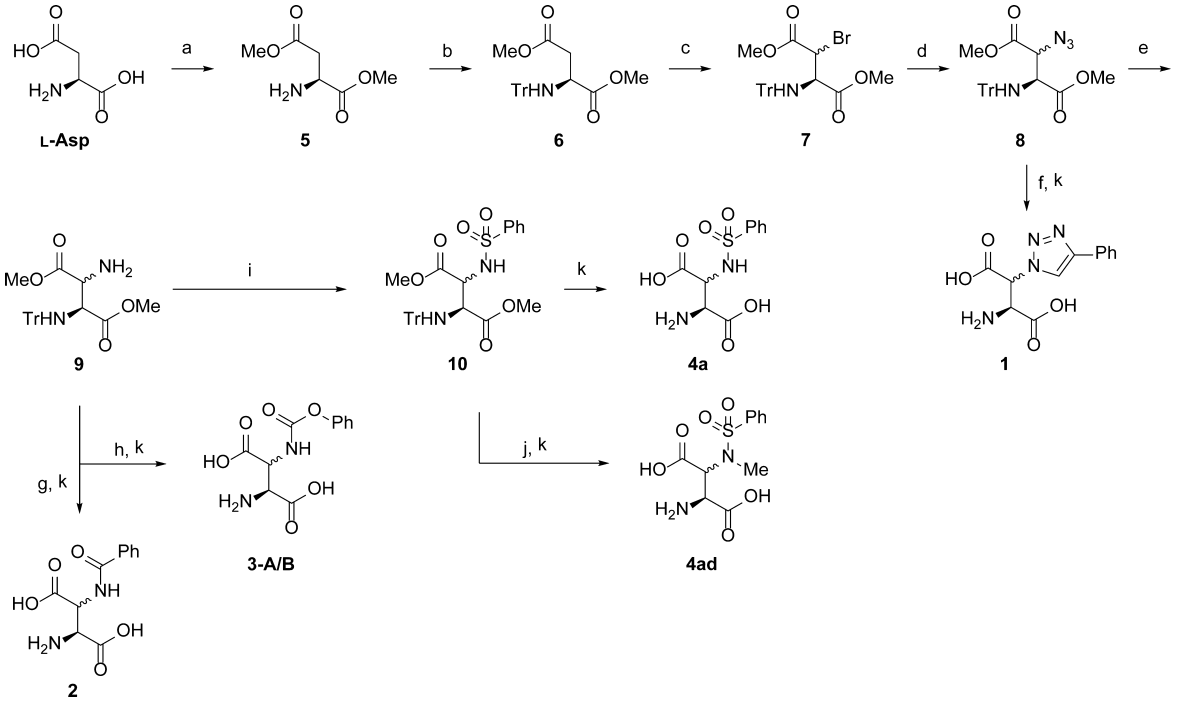

[a]Reagents and conditions: (a) MeOH, H_2SO_4, reflux, quant; (b) TrCl, TEA, DCM, 75% (2 steps); (c) **6**, LHMDS, THF, 30 min, −30 °C, then NBS 100 min, −30 to −5 °C; (d) NaN_3, DMF, 56% (2 steps); (e) PPh_3, THF, 79%; (f) phenylacetylene, sodium ascorbate, $CuSO_4 \cdot 5H_2O$, H_2O/*t*-BuOH; (g) PhCOCl, TEA, DCM; (h) PhOCOCl, TEA, DCM; (i) $PhSO_2Cl$, TEA, DCM; (j) MeI, K_2CO_3, DMF; (k) 6 M HCl, reflux, 1 h, preparative HPLC.

of an sp^2 hybridized nitrogen atom in the β-position of Asp. Furthermore, insertion of an amino group would provide a versatile scaffold, allowing for the synthesis of a variety of derivatives. We therefore nominated β-azido Asp **8** to be a key intermediate in the synthesis of the new β-functionalized Asp analogues.

It has been reported, that differentiation of the *Re* and *Si* face of the in situ formed enolate of *N*-trityl protected Asp ensures diastereoselective insertion of an electrophile at the 3-postion of Asp.[31] A key feature in this stereoselectivity is countercation chelation and temperature. Using LHMDS, the diastereomeric ratio of 1:11 (*S*,*S*:*S*,*R*) is obtained, whereas for KHMDS, a 99:1 (*S*,*S*:*S*,*R*) ratio is achieved. Because the *threo*-diastereomer (TBOA) is the pharmacologically active diastereomer of this class, we planned a *direct* insertion of nitrogen functionality at the β-position using KHMDS. Conversely, *indirect* insertion of nitrogen could be pursued, i.e., suitable S_N2 substitution reaction on the *erythro* intermediate prepared with the use of lithium hexamethyldisilazide (LHMDS).

Initial attempts to functionalize the β-position of Asp were aimed at azidation of dimethyl (2*S*)-*N*-(triphenylmethyl)-aspartate **6** using potassium hexamethyldisilazide (KHMDS) (2.1 equiv) and trisyl-N_3 (2.5 equiv) (Scheme 1). Applying low temperature chelation (−78 °C) failed to produce any conversion. Likewise, elevation of the temperature after addition of electrophilic azidation reagent to 7 °C did not offer any of the desired azide **8**. Increasing the amount of added electrophile and base, for both KHMDS and LHMDS, similarly failed. Confident that the enolate was successfully formed (by quenching with D_2O), we attempted the reaction with less sterically hindered tosyl-N_3, however, this was also unsuccessful.

Because of the apparent lack of reactivity of the azidation reagents toward the enolate, the direct azidation strategy was abandoned. Instead, we turned to the more reactive bromination reagent that could afford the desired 3-bromo Asp **7**, which could then undergo nucleophilic substitution with the sterically less demanding N_3^-. Reaction of NBS with the lithium enolate of **6** (generated with LHMDS) was unreactive at −78 °C but gave full conversion with dr 1:0.3 when warming to rt. Repeating these conditions with Br_2 as the electrophile produced a complex mixture of products, even at −78 °C. We therefore examined the temperature range of reactivity for NBS and found it to be −48 °C to −30 °C under these reaction conditions. Realizing that we could not obtain full diastereoselective control in this reaction step, we decided to aim for a 1:1 mixture of diastereomers. Gratifyingly, full conversion was achieved at −30 to −5 °C to give bromide **7** in diastereomeric ratio 2:3, which was used without further purification. Conversion of crude bromide **7** to azide **8** proceeded smoothly with NaN_3 in anhyd DMF in quantitative yield. To access triazole **1**, azide **8** cleanly underwent copper catalyzed Huisgen cycloaddition, followed by hydrolysis and purification by preparative HPLC to give target compound **1** in 14% yield with dr 0.5:1. Amide **2**, carbamates **3A**-**A**/**B**, and sulfonamide **4a** (Figure 2) were synthesized by first reducing azide **8** to amine **9** under Staudinger conditions followed by reaction with benzoyl chloride, phenyl chloroformate, and phenylsulfonyl chloride, respectively (Scheme 1).

Pharmacological Characterization of 1, 2, 3-A/B, and 4a at EAAT1−3. The pharmacological properties of the four Asp analogues **1**, **2**, **3**-**A**/**B**, and **4a** were characterized at stable EAAT1-, EAAT2-, and EAAT3-HEK293 cells in a conventional [^{3}H]-D-Asp uptake assay,[14] and the results are given in Table 1.

DOI: 10.1021/acs.jmedchem.6b01066
J. Med. Chem. XXXX, XXX, XXX−XXX

Table 1. Pharmacological Properties of Previously Reported Asp Analogues and β-Sulfonamide Asp Analogues at Stable EAAT1-, EAAT2-, and EAAT3-HEK293 Cell Lines in the [^{3}H]-D-Asp Uptake Assay (IC_{50} Values are Given in μM with pIC_{50} ± SEM in Brackets (n = 3−5))

Cmpd no	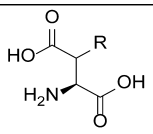	d.r.	EAAT1 IC_{50} (μM) [pIC_{50} ± S.E.M.]	EAAT2 IC_{50} (μM) [pIC_{50} ± S.E.M.]	EAAT3 IC_{50} (μM) [pIC_{50} ± S.E.M.]
TBOA	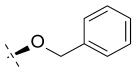	L-*threo*	1.6 [5.79±0.12]	0.96 [6.02±0.05]	3.7 [5.43±0.03]
18	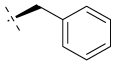	L-*threo*	51 [4.29±0.08]	42 [4.37±0.07]	11 [4.96±0.07]
1	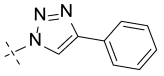	1 : 0.5	>1000 [<3.0]	~500 [a] [~3.3]	>1000 [<3.0]
2	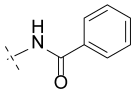	1 : 0.5	~300 [a] [~3.5]	~70 [a] [~4.1]	~1000 [a] [~3.0]
3-A	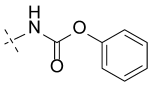	Single Diastereomer	~1000 [a] [~3.0]	>1000 [<3.0]	~300 [a] [~3.5]
3-B	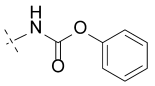	Single diastereomer	~70 [a] [~4.1]	~300 [a] [~3.5]	~300 [a] [~3.5]
4a	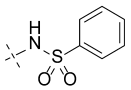	1 : 0.8	2.0 [5.71±0.11]	6.8 [5.17±0.06]	6.2 [5.20±0.09]

[a]Because the concentration−inhibition curves for the compound were not completed within the concentration range tested, the IC_{50} value was estimated based on the fitted curve.

While the 4′-phenyl triazole analogue **1** was inactive as inhibitor at EAAT1−3, the amide **2** displayed weak inhibitory activity at EAAT2 (IC_{50} ~ 70 μM) while being inactive at EAAT1,3 at concentrations up to 300 μM. As for the two diastereomeric carbamate analogues, **3-A** displayed negligible inhibitory activity at EAAT1−3, whereas the other diastereomer **3-B** showed weak inhibitory activity at EAAT1 (IC_{50} ~ 70 μM) and even weaker activity at EAAT2,3. Interestingly, the sulfonamide analogue **4a** displayed significant inhibitory activity at the three transporter subtypes, with IC_{50} values ranging from 2.0 to 6.8 μM.

Stereochemistry of 4a. To address stereochemical reference to **18** and TBOA, the diastereomeric mixture **4a** was separated by preparative HPLC to afford the single diastereomers **4a-A** and **4a-B**. When characterized functionally at EAAT1−3 in the [^{3}H]-D-Asp uptake assay, distinct pharmacological profiles were disclosed for the respective diastereomers. Diastereomer **4a-A** displayed negligible inhibitory activity at EAAT1−3, whereas **4a-B** exhibited inhibitory potencies in the high nanomolar/low micromolar range across the three subtypes (IC_{50} values of 0.80−2.4 μM, Table 2 and Figure 3). To assign the absolute stereochemistry at the β-position of diastereomers **4a-A** and **4a-B**, they were functionalized with $PhSO_2Cl$ at the α-amino group to form the corresponding disulfonamido derivatives (Scheme 2). Hereby, only the *erythro*-diastereomer would acquire a plane of symmetry (*meso* compound) and thus not be optically active. The disulfonamido derivative of the pharmacologically inactive diastereomer **4a-A** was without optical rotatory power and hence assigned the *erythro* configuration, while the disulfonamido derivative of the pharmacologically active diastereomer **4a-B** was optically active and hence unambiguously assigned the L-*threo* isomer (Scheme 2).

Design, Synthesis, and Pharmacological Characterization of Analogues of 4a. Given the interesting pharmacological properties of the sulfonamide analogue **4a-B**, this series was expanded to investigate the influence of substitution on the aryl ring (Table 2). The synthesis of all 28 new analogues followed the strategy outline in Scheme 1 for the synthesis of **4a**, and the pharmacological characterization was performed at the EAAT1-, EAAT2-, and EAAT3-HEK293 cell lines in the [^{3}H]-D-Asp uptake assay.[14]

In comparison with lead structure **4a**, the 1-napthyl (**4b**) and the 2-naphtyl (**4c**) analogues both displayed reduced inhibitory activities at EAAT1−3 (IC_{50} values of 6.5−65 μM). Interestingly though, expansion of the aromatic system in 1-naphthyl Asp derivative **4b** induced a 5-fold preference for EAAT2 over EAAT1,3. Increasing the distance between the

DOI: 10.1021/acs.jmedchem.6b01066
J. Med. Chem. XXXX, XXX, XXX−XXX

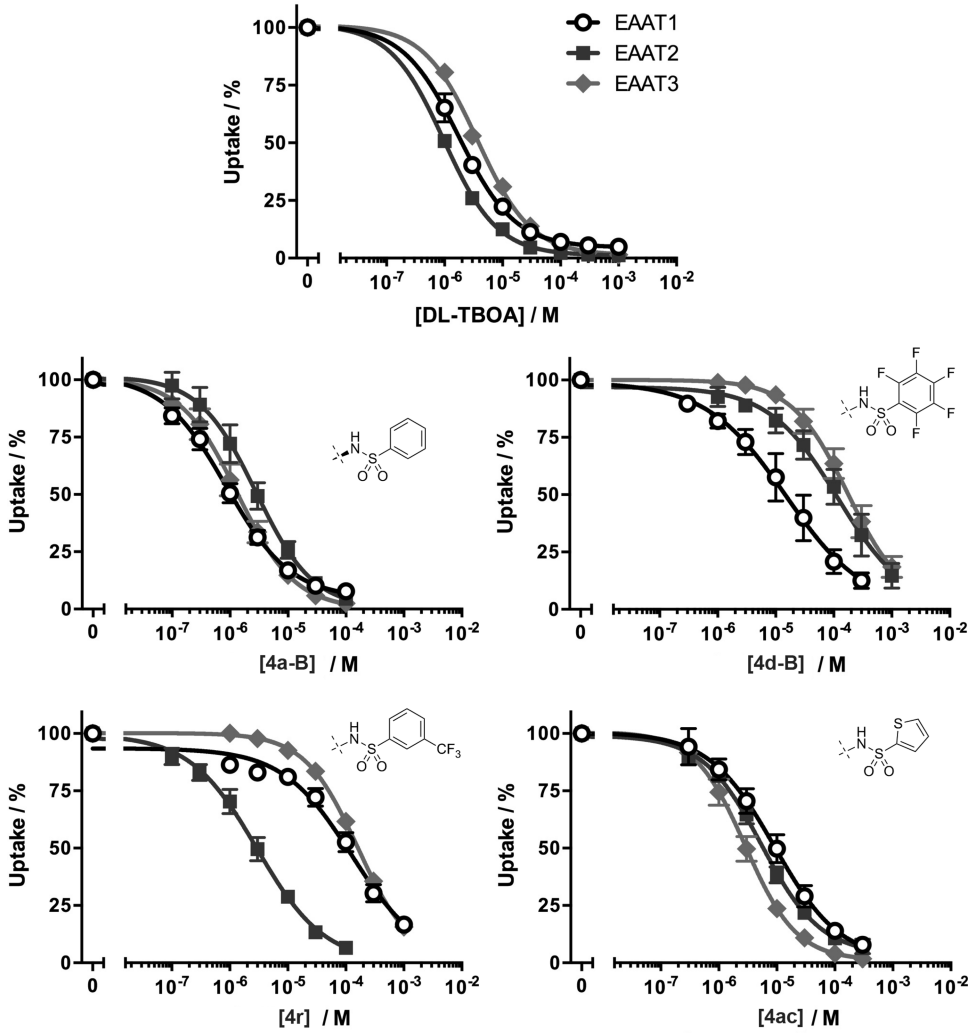

Figure 3. Concentration−inhibition curves for TBOA and β-sulfonamide Asp analogues **4a-B**, **4d-B**, **4r**, and **4ac** at stable EAAT1-, EAAT2-, and EAAT3-HEK293 cell lines in the [^{3}H]-D-Asp uptake assay. Data are given as mean ± SEM (n = 3−5).

Scheme 2. Assignment of Absolute Configurations of the Diastereomers Phenylsulfonamides 4a-A and 4a-B[a]

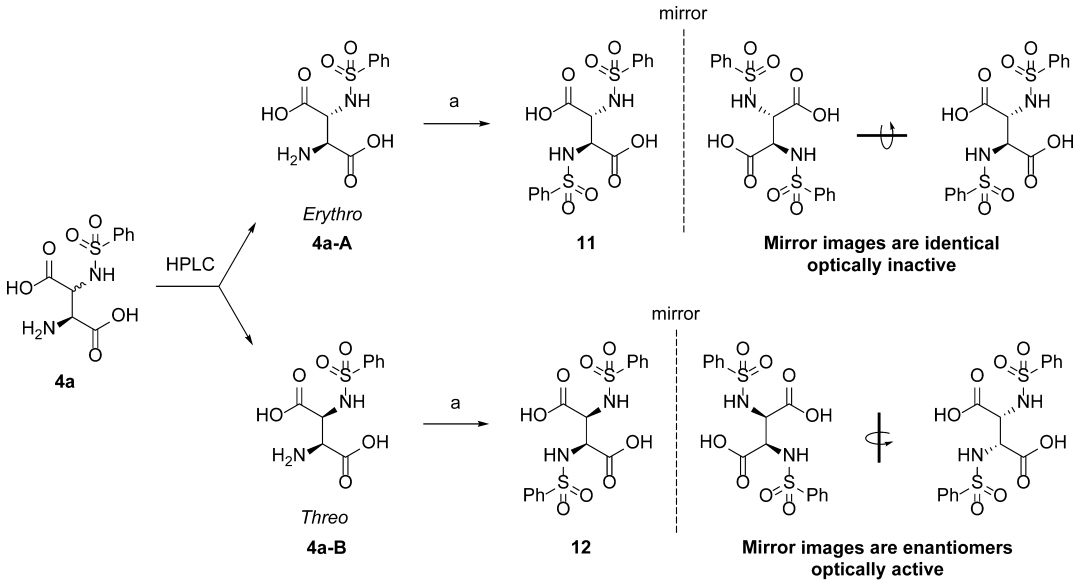

[a](a) $PhSO_2Cl$, NaOH, DIPEA, acetone

DOI: 10.1021/acs.jmedchem.6b01066
J. Med. Chem. XXXX, XXX, XXX−XXX

Table 2. Pharmacological Properties of *β*-sulfonamide Asp Analogues at Stable EAAT1-, EAAT2-, and EAAT3-HEK293 Cell Lines in the [^{3}H]-D-Asp Uptake Assay

Cmpd no	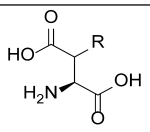	Diastereomeric ratio (d.r.)	EAAT1 IC_{50} (μM) [pIC_{50} ± S.E.M.]	EAAT2 IC_{50} (μM) [pIC_{50} ± S.E.M.]	EAAT3 IC_{50} (μM) [pIC_{50} ± S.E.M.]
4a-A	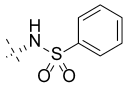	L-*erythro*	~200 [a] [~3.7]	~300 [a] [~3.5]	~300 [a] [~3.5]
4a-B	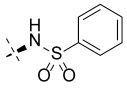	L-*threo*	0.80 [6.10±0.12]	2.4 [5.62±0.15]	1.2 [5.92±0.14]
4b	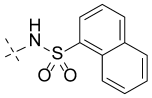	1 : 0.7	65 [4.19±0.04]	14 [4.87±0.09]	63 [4.20±0.05]
4c	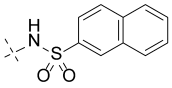	1 : 0.9	8.8 [5.05±0.07]	6.5 [5.19±0.09]	34 [4.47±0.08]
4d-A	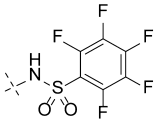	Single diastereomer	>300 [<3.5]	>300 [<3.5]	>300 [<3.5]
4d-B	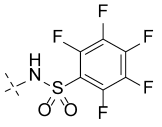	Single diastereomer	16 [4.79±0.19]	~100 [a] [~4.0]	~150 [a] [~3.8]
4e	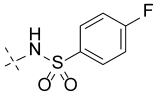	1 : 0.8	1.6 [5.79±0.17]	4.7 [5.33±0.06]	2.0 [5.69±0.04]
4f	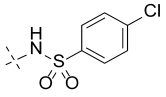	1 : 1	0.32 [6.50±0.20]	3.1 [5.52±0.13]	1.0 [6.01±0.06]
4g	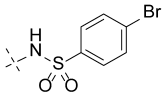	1 : 0.8	0.35 [6.44±0.06]	5.0 [5.31±0.04]	2.6 [5.59±0.03]
4h	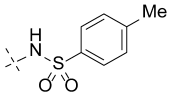	1 : 0.7	0.38 [6.42±0.05]	3.3 [5.49±0.03]	1.9 [5.71±0.04]
4i	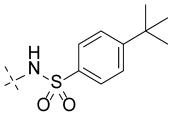	1 : 0.4	~300 [a] [~3.5]	~50 [a] [~4.3]	~300 [a] [~3.5]
4j	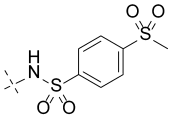	1 : 1	~300 [a] [~3.5]	~300 [a] [~3.5]	~300 [a] [~3.5]
4k	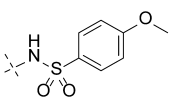	1 : 0.7	4.0 [5.39±0.06]	~30 [a] [~4.5]	~30 [a] [~4.5]

DOI: 10.1021/acs.jmedchem.6b01066
J. Med. Chem. XXXX, XXX, XXX−XXX

Table 2. continued

Cmpd no	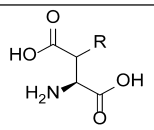	Diastereomeric ratio (d.r.)	EAAT1 IC_{50} (μM) [pIC_{50} ± S.E.M.]	EAAT2 IC_{50} (μM) [pIC_{50} ± S.E.M.]	EAAT3 IC_{50} (μM) [pIC_{50} ± S.E.M.]
4l	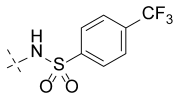	1 : 0.7	~30 [a] [~4.5]	~50 [a] [~4.3]	~100 [a] [~4.0]
4m	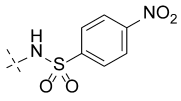	1 : 0.8	13 [4.89±0.04]	~50 [a] [~4.3]	~100 [a] [~4.0]
4n	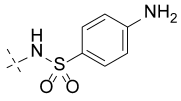	1 : 0.8	2.3 [5.63±0.21]	4.7 [5.33±0.04]	3.0 [5.53±0.13]
4o	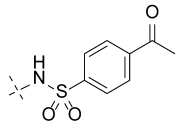	1 : 0.6	44 [4.36±0.10]	43 [4.37±0.05]	~100 [a] [~4.0]
4p	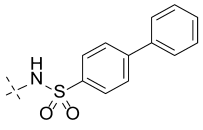	1 : 0.4	2.3 [5.65±0.04]	0.50 [6.30±0.02]	20 [4.69±0.07]
4q	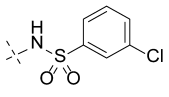	1 : 0.8	3.8 [5.42±0.05]	2.7 [5.57±0.15]	12 [4.92±0.07]
4r	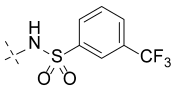	1 : 0.7	~100 [a] [~4.0]	2.8 [5.56±0.11]	~150 [a] [~3.8]
4s	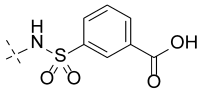	1 : 0.9	>300 [<3.5]	>300 [<3.5]	>300 [<3.5]
4t	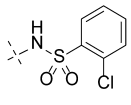	1 : 0.9	1.7 [5.76±0.15]	3.3 [5.48±0.11]	6.5 [5.19±0.04]
4u	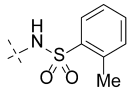	1 : 0.7	2.7 [5.56±0.15]	6.6 [5.18±0.06]	8.8 [5.06±0.11]
4v	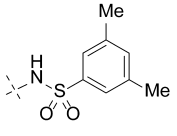	1 : 0.8	63 [4.20±0.10]	11 [4.97±0.12]	~100 [a] [~4.0]
4x	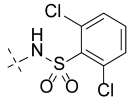	1 : 0.7	~100 [a] [~4.0]	~50 [a] [~4.3]	~300 [a] [~3.5]

DOI: 10.1021/acs.jmedchem.6b01066
J. Med. Chem. XXXX, XXX, XXX−XXX

Table 2. continued

Cmpd no		Diastereomeric ratio (d.r.)	EAAT1 IC_{50} (μM) [pIC_{50} ± S.E.M.]	EAAT2 IC_{50} (μM) [pIC_{50} ± S.E.M.]	EAAT3 IC_{50} (μM) [pIC_{50} ± S.E.M.]
4y	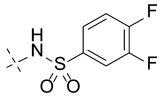	1 : 0.8	0.80 [6.10±0.06]	11 [5.96±0.04]	7.4 [5.13±0.05]
4z	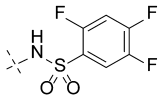	1 : 0.8	2.5 [5.60±0.15]	22 [4.65±0.08]	10 [4.98±0.11]
4aa	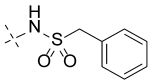	1 : 0.9	49 [4.31±0.01]	60 [4.22±0.03]	76 [4.12±0.09]
4ab	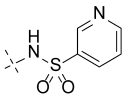	1 : 0.3	18 [4.74±0.08]	28 [4.60±0.04]	13 [4.12±0.09]
4ac	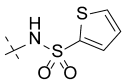	1 : 0.9	9.4 [5.03±0.13]	7.3 [5.14±0.02]	3.1 [5.51±0.10]
4ad	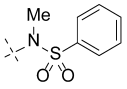	1 : 0.7	>300 [<3.5]	>300 [<3.5]	>300 [<3.5]

[a]Because the concentration−inhibition curves for the compound were not completed within the concentration range tested, the IC_{50} value was estimated based on the fitted curve.

Asp backbone and the aromatic group in the benzyl derivative **4aa** also failed to increase the inhibitory potency (IC_{50} values of 49−76 μM), and as with the lead **4a**, no subtype selectivity was observed for this analogue.

Extending the study of the aromatic group to include heteroaromatic analogues **4ab** and **4ac** gave further insight into the biologically active space for this ligand series. The two analogues were essentially nonselective inhibitors of EAAT1−3, with the 2-thiophene analogue **4ac** being roughly equipotent with **4a**-**B** at the transporters. Interestingly, however, **4ac** displayed a slightly lower (~3-fold) IC_{50} value at EAAT3 than at EAAT1,2 (Table 2 and Figure 3). Although this difference is too small to classify the analogue as an EAAT3-preferring inhibitor, the fairly high inhibitory potency and EAAT1−3 profile of **4ac** suggests that it could be a potential lead structure for the future development of EAAT3-preferring or -selective inhibitors.

The synthesis and pharmacological characterization of the *N*-methylated analogue **4ad** again demonstrated that subtle chemical changes to a ligand may completely eliminate pharmacological activity. The analogue **4ad** was without inhibitory activity at all three EAATs (IC_{50} values >300 μM). Rotational restriction of the phenyl ring by introduction of two *ortho*-chloro atoms, compound **4x**, also decreased the inhibitory EAAT potency significantly (IC_{50} values of 50−300 μM) in comparison to the lead structure **4a**.

We were intrigued to investigate the possibility of a π−cation interaction between the phenyl ring in the lead structure **4a** and the substrate binding pocket in the EAAT. Hence, the pentafluorophenyl derivative **4d** was synthesized.[32] As for lead structure **4a**, the diastereomers of **4d** were easily separated into diastereomer **4d**-**A** and diastereomer **4d**-**B**. In agreement with lead structure **4a**, the inhibitory activity resided only in the single diastereomer **4d**-**B**, which was shown to be an EAAT1-preferring inhibitor, exhibiting an IC_{50} value of 16 μM at EAAT1 and 6-fold and 10-fold lower inhibitory potencies at EAAT2 and EAAT3, respectively (Table 2 and Figure 3). Considering the differences in inhibitory potencies across EAAT1−3, the putative π−cation is either manifested differently between EAAT subtypes, or alternatively the difference in the pharmacological profiles of **4d**-**B** and **4a**-**B** is a direct effect of the fluorine substitution.

To gain further insight into the impact that pentafluorination of the phenyl ring had on EAAT potency and subtype selectivity, the mono-, di-, and trifluoro analogues **4e**, **4y**, and **4z** were synthesized. Analogously to pentafluorinated analogue **4d**-**B**, the 2,4,5-trifluorinated analogue **4z** displayed preference for EAAT1 over EAAT2 and EAAT3 (9- and 4-fold, respectively), and moreover it exhibited a 6-fold increase in inhibitory potency for EAAT1 compared to **4d**-**B**. Interestingly, the 3,4-difluorinated analogue **4y** again incrementally increased inhibitory potency toward EAAT1 by 3-fold (IC_{50} 0.80 μM), and furthermore this analogue exhibited an even more pronounced preference for EAAT1 over EAAT2 (14-fold) and EAAT3 (9-fold) (Table 2). The 4-fluoro analogue **4e** displayed similar inhibitory potency at EAAT1 (IC_{50} 1.6 μM) as

DOI: 10.1021/acs.jmedchem.6b01066
J. Med. Chem. XXXX, XXX, XXX−XXX

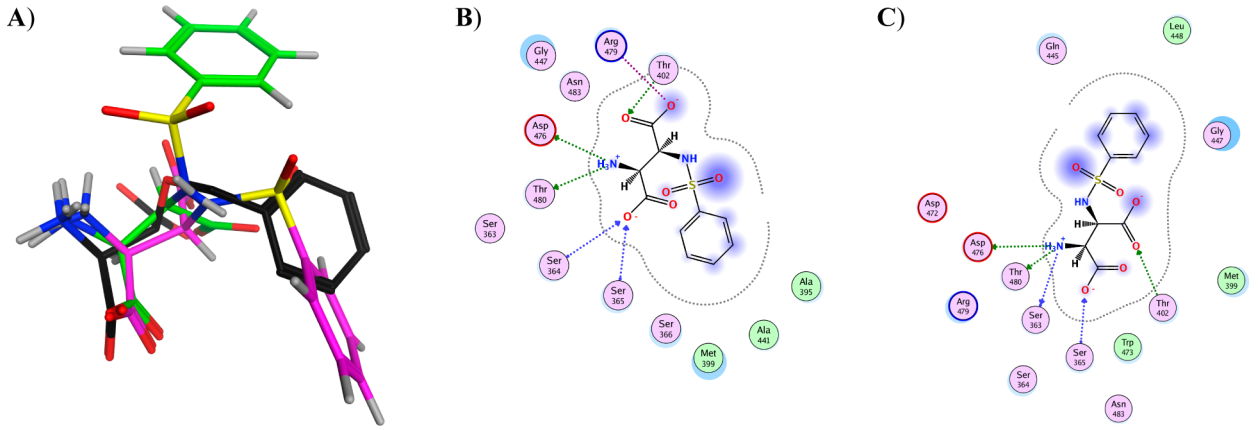

Figure 4. (A) Superimposition of binding mode of TBOA (black) when crystallized in Glt_{Ph} (PDB code: 2nww) with the two most favorable binding modes of **4a-B** (magenta and green) obtained by docking into a homology model of EAAT1 built from the Glt_{Ph}/TBOA crystal structure.[36] (B) Binding of magenta **4a-B** in EAAT1. (C) Binding of green **4a-B** in EAAT1.

4y, but in contrast to **4y** it was essentially nonselective at the three EAAT subtypes (IC_{50} values of 1.6−4.7 μM). Thus, the di-, tri-, and pentafluoro derivatives **4y**, **4z**, and **4d-B** all displayed similar degrees of selectivity for EAAT1 over EAAT2,3, whereas reducing the number of fluorine atoms increased the inhibitory potency of the analogues at all three transporter subtypes. However, because the EAAT1-preference of the 3,4-difluoro analogue **4y** was eliminated in the 4-fluoro analogue **4e**, we concluded that a fluoro atom in the 3-position could be essential for this preference. The study of the four fluorinated analogues did not disclose clear evidence for a π−cation interaction, as no correlation of reduced potency with reducing number of fluoro atoms was observed.[33]

To explore in greater details the effects of substituents on the aromatic ring, we then synthesized a number of *ortho*-, *meta*-, and *para*-substituted analogues (Table 2). The *ortho*-Cl analogue **4t** and *ortho*-Me analogue **4u** showed similar pharmacological characteristics as the lead **4a**, with low micromolar inhibitory potencies at all three transporters.

The *para*-position was first probed with the *para*-CF_3 analogue **4l**, which interestingly displayed a significant loss of EAAT activity (IC_{50} values of 30−100 μM). In view of the high inhibitory potencies exhibited by *para*-fluoro analogue **4e** (IC_{50} values of 1.6−4.7 μM) and *para*-Cl analogue **4f** (IC_{50} values of 0.32−3.1 μM), we synthesized the *para*-bromo analogue **4g**. This analogue, however, displayed a similar pharmacological profile (IC_{50} values of 0.35−5.0 μM) to these smaller halide analogues. It was unclear why the *para*-CF_3 analogue **4l** showed weak inhibitory EAAT potency despite having an electronegativity between those of Cl and Br.[34] Thus, we synthesized derivatives **4o**, **4m**, and **4j** to characterize the effects of resonance electron withdrawing. The bulky sulfone analogue **4j** was essentially inactive at EAAT1−3, indicating a possible spatial restriction in the *para*-position. The conjugated ketone analogue **4o** displayed weak, nonselective EAAT inhibition (IC_{50} values of 43−100 μM), while the *para*-NO_2 derivative **4m** exhibited moderate inhibitory activity at EAAT1 (IC_{50} 13 μM) and a small preference for this subtype over EAAT2,3 (Table 2). Thus, inhibitory potency seems not exclusively to be a result of electronic effects, and other factors may play a defining role as well. This lack of correlation is further exemplified when examining electron donating derivatives **4k** and **4n**. While both analogues display low micromolar inhibitory potencies at EAAT1 (IC_{50} values of 4.0 and 2.3 μM, respectively), the aniline analogue **4n** exhibits equipotent inhibition at EAAT2 and EAAT3, whereas the anisole analogue **4k** loses inhibitory potency at these subtypes (IC_{50} values of ∼30 μM). Finally, in an attempt to define the spatial limitations of the *para*-substituent, analogues **4h**, **4i**, and **4p** were synthesized. Here, the steric bulk of the *para*-*tert*-butyl substituent in **4i** almost completely eliminated EAAT activity, analogously to what was observed with the *para*-sulfone analogue **4j**. As with the sterically similar halides, the *para*-Me analogue **4h** displayed potent, albeit nonselective, EAAT inhibition. Highly interestingly, the sterically demanding *para*-biphenyl analogue **4p** displayed high inhibitory potency at EAAT1 and EAAT2 (IC_{50} values of 2.3 and 0.50 μM, respectively) and 10−40-fold lower potency at EAAT3. This selectivity profile is somewhat similar to that exhibited by the 2-naphthyl analogue **4c** (Table 2), and it demonstrates that the EAAT protein is flexible when stressed by a *para*-substituent substantial in size.

In regard to the *meta*-position, the *meta*-CF_3 substituted analogue **4r** displayed a highly interesting selectivity profile at EAAT1−3, being a potent inhibitor of EAAT2 (IC_{50} 2.8 μM) with 30- and 50-fold selectivity toward EAAT1 (IC_{50} ∼ 100 μM) and EAAT3 (IC_{50} ∼ 150 μM), respectively (Table 2 and Figure 3). Interesting, the 3,5-dimethyl analogue **4v** exhibited 5−9-fold preference for EAAT2 over EAAT1,3, and thus the selectivity profiles of these two analogues strongly suggested that the *meta*-position in the phenyl ring is a hot spot for EAAT2-selectivity. Supplementing these findings was the complete loss of EAAT activity observed for the *meta*-COOH analogue **4s** and the fact that the *meta*-Cl analogue **4q** was a potent EAAT1,2-preferring inhibitor. Hence, the identity of the substituent introduced in the *meta*-position of the phenyl ring in the β-sulfonamide Asp analogue is clearly of key importance for its functional properties, both when it comes to its basic EAAT activity but also in terms of whether it exhibits EAAT2-selectivity or not.

Pharmacological Characterization of Selected β-Sulfonamide Asp Analogues at Ionotropic Glutamate Receptors. The β-sulfonamide Asp analogues **4a-A**, **4a-B**, **4b**, **4c**, **4e**, **4h**, **4v**, **4r**, **4f**, **4q**, and **4t** were characterized in radioligand binding assays to native ionotropic glutamate receptors (rat synaptosomes).[35] None of the 11 analogues exhibited significant binding affinity to AMPA receptors ([^{3}H]AMPA displacement), kainic acid receptors ([^{3}H]kainic acid displacement), or NMDA receptors ([^{3}H]-(*R*,*Z*)-2-amino-

DOI: 10.1021/acs.jmedchem.6b01066
J. Med. Chem. XXXX, XXX, XXX−XXX

4-(phosphonomethyl)hept-3-enoic acid ([^{3}H]CGP39653) displacement) when tested at concentrations up to 100 μM.

Modeling. Homology models of EAAT1−3 were built from the crystal structure of Glt_{Ph} crystallized with TBOA (PDB code: 2nww)[36] based on an alignment of the amino acid sequences of the three human transporters and that of Glt_{Ph} (Supporting Information). Subsequently, a docking study was performed of the selected ligands **4a-B** (nonselective), **4d-B** (EAAT1-preferring), **4r** (EAAT2-selective), **4p** (EAAT1,2-preferring), **4ac** (nonselective), and **4ad** (inactive). Unfortunately, this in silico study did not shed further light on the observed differences in pharmacological profiles of the analogues with respect to amino acid residues differing between the substrate binding pocket in EAAT1−3. However, two energetically similar binding modes of **4a-B** were disclosed (Figure 4). The one binding mode of **4a-B** (Figure 4A,B, magenta) very much resembles the binding mode of TBOA in the Glt_{Ph} crystal structure, showing occupancy of a large area in space. The other binding mode of **4a-B** (Figure 4A,C, green) orients the phenyl ring into a different cavity of the substrate binding pocket. Future SAR studies of the β-sulfonamide Asp analogue scaffold may unequivocally conclude which of the two binding modes is the biologically active one or whether both binding modes are possible with preference depending on the specific analogue.

CONCLUSION

In the present study, we have explored new β-functionalized Asp analogues (Table 1) as inhibitors of the EAATs. An elaborate SAR study on the new and potent β-sulfonamide Asp scaffold **4a** was carried out by the synthesis of 28 analogues, and thereby new pharmacological tools for the EAATs were identified. Furthermore, we have highlighted the existence of an adjacent vestibule to the substrate binding site in the transporters that could be highly interesting for future ligand development.

Several analogues of **4a-B** were potent nonselective inhibitors which displayed IC_{50} values in the high-nanomolar/low-microlar range at all three transporters (**4f**, **4g**, and **4h**, Table 2). However, the main objective of this study was to discover subtype-selective or subtype-preferring EAAT inhibitors, and introduction of fluorine atoms on the phenyl ring did indeed yield analogues characterized by preference for EAAT1 over EAAT2,3 (**4d-B**, **4z**, and **4y**). The 3,4-difluoro analogue **4y**, a potent EAAT1 inhibitor (IC_{50} 0.8 μM) displaying 14- and 9-fold preference for this subtype over EAAT2 and EAAT3, respectively, is particularly interesting, as it to the best of our knowledge is the most EAAT1-selective competitive non-substrate inhibitor to be published to date. Even though its EAAT1-preference admittedly pales in comparison with the >300-fold EAAT1-selectivity exhibited by the noncompetitive inhibitors **15**[21] and **16**,[22] we nevertheless find **4y** a promising lead for future development of truly EAAT1-selective inhibitors acting through the substrate-binding site in the transporter.

Another highly interesting analogue to come out of the SAR study was **4r**, obtained by installation of a trifluoromethyl group in the *meta*-position of the phenyl ring. **4r** is a potent EAAT2 inhibitor (IC_{50} 2.8 μM) characterized by ≥30-fold selectivity toward EAAT1 and EAAT3. While this EAAT2-selectivity is substantially lower than that previously reported for WAY-213613, it is roughly comparable to those exhibited by DHK and **13**, and it should also be noted that **4r** is 10−30-fold more potent at EAAT2 than these two latter inhibitors.[14−17] Moreover, considering the relatively limited SAR work focused on the *meta*-position in the phenyl ring of the β-sulfonamide Asp analogue performed in the present study, it seems plausible that future medicinal chemistry development based on **4r** as lead could provide analogues with further increased inhibitory potencies and/or degrees of EAAT2-selectivity.

This SAR study also elucidates the existence of an adjacent vestibule to the substrate binding site in the EAAT that holds considerable promise for future development of transporter ligands. Collectively, the EAAT1-preferences and EAAT2-selectivities exhibited by analogues in this series, the EAAT3-preference reported for **18**,[25] and the completely nonselective EAAT inhibition mediated by TBOA[14,15] and other analogues from this series illustrate the apparently immense potential for functional diversity in Asp analogues with 3-substituents projecting into this adjacent vestibule. Although we were unable to rationalize the molecular basis for the different selectivity profiles displayed by the β-sulfonamide Asp analogues in our in silico study, we propose that Asp analogues comprising 3-substituents with even slightly different spatial orientations could exhibit very different selectivity profiles at the EAATs, and future studies applying this strategy could thus perhaps help to supplement the presently limited selection of pharmacological tools in the field.

EXPERIMENTAL SECTION

Chemistry. All reactions involving dry solvents or sensitive agents were performed under an argon atmosphere, and glassware was flame-dried under vacuum prior to use. Commercially available chemicals were used without further purification with the exception of *N*-bromosuccinimide (NBS), which was recrystallized from water and lyophilized to produce a white flaky solid. DCM, THF, and DMF were dried using a SG WATER solvent purification system (commercialized by Pure Process Technology). MeOH was dried by standing over 4 Å molecular sieves for a minimum of 48 h. Triethylamine (TEA) was purified by fractional distillation, followed by standing over 4 Å molecular sieves. Reactions were monitored by analytical thin-layer chromatography (TLC, Merck silica gel 60 F_{254} aluminum sheets) or by HPLC.

Flash chromatography was carried out using Merck silica gel 60A (40−63 μm). For dry column vacuum chromatography (DCVC), Merck silica gel 60 (15−40 μm) and a standard setup was used.

^{1}H NMR spectra were recorded at 400 or 600 MHz and ^{13}C NMR spectra at 100 or 150 MHz on a Bruker Avance III or Bruker Avance III HD, respectively. Chemical shifts (δ) are reported in ppm relative to TMS. For ^{13}C NMR in D_2O was added 1% MeOD as internal reference. ^{19}F NMR spectra were recorded using $CFCl_3$ as reference standard.

HPLC was performed using a Dionex UltiMate 3000 pump and photodiode array detector (210 and 254 nm, respectively) installed with an XTerra MS C 18 3.5 μ m, 4.6 mm × 150 mm column, using a 5 → 95% MeCN gradient in H_2O containing 0.1% TFA. For HPLC control, data collection, and data handling, Chromeleon software v. 6.80 was used. Preparative HPLC was carried out on an Agilent Prep HPLC systems with Agilent 1100 series pump, Agilent 1200 series diode array, multiple wavelength detector (G1365B), and Agilent PrepHT High Performance Preparative Cartridge Column (Zorbax, 300 SB-C18 Prep HT, 21.2 mm × 250 mm, 7 μm). LC-MS spectra were recorded using either an Agilent 1200 series solvent delivery system equipped with an autoinjector coupled to an Agilent 6400 series triple quadrupole mass spectrometer equipped with an electrospray ionization source or Waters Aquity UPLC-MS with dual wavelength detection with electrospray ionization. Gradients of 5% aqueous MeCN + 0.1% HCO_2H (solvent A) and 95% aqueous MeCN + 0.05% HCO_2H (solvent B) were employed. IR spectra were recorded on a PerkinElmer 801 spectrophotometer. Optical rotation was measured using a PerkinElmer 241 spectrometer, with Na lamp

DOI: 10.1021/acs.jmedchem.6b01066
J. Med. Chem. XXXX, XXX, XXX−XXX

(D line, 589 nm). Compounds were dried under high vacuum or freeze-dried using a Holm & Halby, Heto LyoPro 6000 freeze drier. The purity of compounds submitted for pharmacological characterization was determined by LCMS to be >95%.

General Procedure for Synthesis and Purification of Sulfonamide Aspartate Analogues (General Procedure A). In a representative reaction, a dry, argon-filled 20 mL vial, fitted with screw-cap and PTFE/silicone septum and magnetic stirrer, for 18 h was charged with dimethyl (2*S*)-3-amino-*N*-(triphenylmethyl)-aspartate **9** (200 mg, 478 μmol) and anhydrous DCM (6 mL). To the stirred solution was added TEA (100 μL, 717 μmol) and the desired arylsulfonyl chloride, respectively. The mixture was stirred at ambient temperature for 20 h and then diluted with DCM (2 mL). The reaction mixture was washed once with 1 M HCl and three times with saturated $NaHCO_3$ by addition of the aqueous solution to the vial, agitating, and removing the aqueous layer with a pipet. The organic phase was reduced under a stream of air, followed by evaporation in vacuo. The residue was used in the following step without further purification.

The crude, protected sulfonamide aspartate analogue was suspended in 6 M HCl (5 mL). The capped vial was stirred vigorously at 100 °C for 4.5 h and then allowed to cool to room temperature. The reaction mixture was then washed three times with Et_2O and three times with DCM, and the aqueous phase was concentrated in vacuo. The residue was taken up in a minimum of H_2O (0.1% TFA) and purified on a preparative HPLC. Fractions were analyzed by LC-MS or NMR (0.5 mL sample from tube + 0.05 mL D_2O) and collected accordingly. The combined fractions were sequentially concentrated and then added 1 M HCl (5 mL), after which the compounds were lyophilized.

Alternative Procedure for the Synthesis and Purification of Sulfonamide Aspartate Analogues (General Procedure B). In cases of large amounts of arylsulfonate byproduct, an alternative procedure was used. The desired aspartate analogue was synthesized and hydrolyzed as described in general procedure A. Following the wash of the aqueous hydrolysate with Et_2O and DCM, the solution was subjected to ion exchange chromatography. A filter with a sintered glass frit was filled with Amberlite IRA-420 (2 cm × 7 cm). The funnel was assembled with a separation funnel and an adapter with side arm, resembling a setup for dry column vacuum chromatography. The column was pre-equilibrated with 1 M HCl until the effluent was at pH = 1. The hydrolysate was charged to the resin and passed through the column with 1 M HCl (20 mL) by applying a very slight vacuum. The resulting effluent was collected in a 100 mL round-bottom flask, evaporated, and purified by preparative HPLC.

Symmetrization of 4a-A and 4a-B for Elucidation of Absolute Stereochemistry. Each of the purified and separated diastereomers, **4a-A** and **4a-B** (3.15 mg, 9.7 μmol), were dissolved in NaOH (29 μL, 1 M aq, 29 μmol) in separate Eppendorf tubes at 0 °C. Benzenesulfonyl chloride (1.4 μL, 10.7 μmol), *N*,*N*-diisopropylethylamine (1.9 μL, 10.7 μmol), and acetone (10 μL) were added, and the reaction mixture was allowed to warm to room temperature over 2 h and stirred for an additional 16 h. Each of the reaction mixtures were then diluted with 1 mL of H_2O and purified by preparative HPLC to produce **11** (2.05 mg, 49%, from **4a-A**) and **12** (inseparable 2:3 ratio with benzenesulfonate, from **4a-B**). Optical rotation was measured in triplicate for each of the samples, and only **12** was able to perform rotation (in 1 mL of distilled MeOH, at 20 °C; cuvette, 10 cm, α = 0.03 for **12**). **11**: ^{1}H NMR (600 MHz, CD_3OD) δ: 7.86−7.82 (m, 4H), 7.61 (td, J = 7.3, 1.3 Hz, 2H), 7.55−7.51 (m, 4H), 4.24 (s, 2H). **12**: ^{1}H NMR (600 MHz, CD_3OD) δ: 7.84−7.79 (m, 4H), 7.59 (dd, J = 7.4, 1.2 Hz, 2H), 7.54−7.47 (m, 4H), 4.41 (s, 2H). **11**: ^{13}C NMR (151 MHz, CD_3OD) δ: 170.6, 141.7, 133.8, 130.1, 128.4, 59.6. **12**: ^{13}C NMR (151 MHz, CD_3OD) δ: 170.7, 141.8, 133.8, 130.0, 128.2, 59.3.

(2S)-3-(4-Phenyl-1H-1,2,3-triazol-1-yl)aspartic Acid (1). Dimethyl (2*S*)-3-azido-*N*-(triphenylmethyl)aspartate (**8**) (150 mg, 338 μmol) and phenylacetylene (78 μL, 709 μmol) were suspended in H_2O/*t*-BuOH (1.35 mL 1:1 v/v) in a vial. Sodium ascorbate (33 μL, 1 M aq, 34 μmol) was added, followed by $CuSO_4 \cdot 5H_2O$ (114 μL, 0.3 M aq, 34 μmol), and the reaction mixture was stirred at ambient temperature for 16 h under argon. The reaction mixture was diluted with H_2O and extracted three times with Et_2O. The combined organic extracts were concentrated in vacuo and directly suspended in 6 M HCl (5 mL) and subsequently refluxed for 4 h. The cooled aqueous reaction mixture was washed twice with Et_2O, concentrated in vacuo, and purified twice by preparative HPLC. The combined were evaporated, and 1 M HCl (5 mL) was added and evaporated. This was repeated three times to give the HCl salt of **1** (13 mg, 14% from **8**, diastereomeric ratio 0.5:1). Diastereomer 1: ^{1}H NMR (400 MHz, DMSO-d_6) δ: 8.80 (broad s, 3H), 8.65 (s, 1H), 7.83 (d, J = 7.6 Hz, 2H), 7.46 (t, J = 7.6 Hz, 2H), 7.40−7.30 (m, 1H), 6.21 (d, J = 4.4 Hz, 1H), 4.85 (d, J = 4.4 Hz, 1H). Diastereomer 2: ^{1}H NMR (400 MHz, DMSO-d_6) δ: 8.80 (s, 3H), 8.51 (s, 1H), 7.83 (d, J = 7.6 Hz, 2H), 7.46 (t, J = 7.6 Hz, 2H), 7.40−7.30 (m, 1H), 6.18 (d, J = 3.7 Hz, 1H), 4.91 (d, J = 3.7 Hz, 1H). Diastereomer 1: ^{13}C NMR (101 MHz, DMSO-d_6) δ: 167.5, 166.5, 146.4, 130.3, 129.1, 128.3, 125.4, 123.2, 61.3, 53.0. Diastereomer 2: ^{13}C NMR (101 MHz, DMSO-d_6) δ: 167.4, 166.4, 146.2, 130.4, 129.1, 128.2, 125.3, 123.6, 61.2, 52.8. LCMS (ES+) m/z 277.0 $[M + H]^+$, $C_{12}H_{13}N_4O_4$ requires 277.1.

(2S)-3-Benzamidoaspartic Acid (2). Dimethyl (2*S*)-3-amino-*N*-(triphenylmethyl)aspartate **9** (150 mg, 358 μmol) was dissolved in anhydrous DCM (4.5 mL) in a dry flask under argon. The solution was cooled to 0 °C followed by addition of TEA (75 μL, 537 μmol) and benzoyl chloride (50 μL, 430 μmol), and the solution was allowed to reach ambient temperature. The solution was stirred for 3 days, evaporated, and resuspended in 5 mL of 6 M HCl and refluxed for 4 h. The resulting mixture was concentrated in vacuum and purified by preparative HPLC (combined fractions were evaporated, 1 M HCl (5 mL) added, and concentrated). This was repeated three times to produce the HCl salt to give **2** as a colorless solid (26 mg, 29% from **9**, diastereomeric ratio 0.5:1). Diastereomer 1: ^{1}H NMR (600 MHz, D_2O) δ: 7.73 (ddd, J = 8.3, 6.6, 1.3 Hz, 2H), 7.59−7.53 (m, 1H), 7.45 (td, J = 7.9, 1.4 Hz, 2H), 5.24 (d, J = 3.5 Hz, 1H), 4.66 (d, J = 3.5 Hz, 1H). Diastereomer 2: ^{1}H NMR (600 MHz, D_2O) δ: 7.73 (ddd, J = 8.3, 6.6, 1.3 Hz, 2H), 7.59−7.53 (m, 1H), 7.45 (td, J = 7.9, 1.4 Hz, 2H), 5.16 (d, J = 3.5 Hz, 1H), 4.57 (d, J = 3.5 Hz, 1H). Diastereomer 1: ^{13}C NMR (151 MHz, D_2O) δ: 172.60, 171.52, 169.88, 133.82, 133.10, 129.74, 128.48, 56.19, 53.79. Diastereomer 2: ^{13}C NMR (151 MHz, D_2O) δ: 172.25, 171.95, 170.50, 133.86, 132.97, 129.79, 128.38, 55.28, 53.58. LCMS (ES+) m/z 253.2 $[M + H]^+$, $C_{11}H_{13}N_2O_5$ requires 253.1.

(2S)-3-((Phenoxycarbonyl)amino)aspartic Acid (3-A). Dimethyl (2*S*)-3-amino-*N*-(triphenylmethyl)aspartate **9** (150 mg, 358 μmol) was dissolved in 4.5 mL of anhydrous DCM in a dry flask under argon followed by addition of TEA (75 μL, 537 μmol) and phenyl chloroformate (54 μL, 439 μmol). The reaction mixture was stirred at room temperature for 18 h and then concentrated in vacuo. The crude residue was suspended in 6 M HCl (5 mL) and refluxed for 4 h. The cooled mixture was washed twice with Et_2O, concentrated, and purified by preparative HPLC to yield single diastereomer (22 mg, 23% from **9**) after sequential evaporation from 5 mL of 1 M HCl (three times). One single diastereomer: ^{1}H NMR (400 MHz, DMSO-d_6) δ: 8.66 (s, 3H), 8.34 (d, J = 9.4 Hz, 1H), 7.45−7.36 (m, 2H), 7.28−7.20 (m, 1H), 7.20−7.12 (m, 2H), 4.85 (dd, J = 9.4, 3.4 Hz, 1H), 4.40 (d, J = 3.8 Hz, 1H). ^{13}C NMR (101 MHz, DMSO-d_6) δ: 169.0, 167.6, 154.8, 150.8, 129.3, 125.3, 121.6, 53.9, 53.8. LCMS (ES+) m/z 269.2 $[M + H]^+$, $C_{11}H_{12}N_2O_6$ requires 269.1.

(2S)-3-((Phenoxycarbonyl)amino)aspartic Acid (3-B). Diastereomer **3-B** was isolated as impure fractions from preparative HPLC in **3-A**. These concentrated fractions were subsequently purified by a second preparative HPLC run to give **3-B** (15 mg, 16% from **9**) after three sequential evaporations from 1 M HCl (5 mL). One single diastereomer: ^{1}H NMR (400 MHz, DMSO-d_6) δ: 8.75 (s, 3H), 8.31 (d, J = 9.3 Hz, 1H), 7.47−7.34 (m, 2H), 7.29−7.17 (m, 1H), 7.15−7.07 (m, 2H), 4.77 (dd, J = 9.3, 4.6 Hz, 1H), 4.37 (d, J = 4.6 Hz, 1H). ^{13}C NMR (101 MHz, DMSO-d_6) δ: 169.3, 168.2, 154.4, 150.8, 129.4, 125.4, 121.6, 53.8, 53.1. LCMS (ES+) m/z 269.0 $[M + H]^+$, $C_{11}H_{12}N_2O_6$ requires 269.1.

(2S,3R)-3-(Phenylsulfonamido)aspartic Acid (4a-A). General procedure A. Yield 17 mg, 15%. ^{1}H NMR (400 MHz, DMSO-d_6) δ: 8.66 (br s, 3H), 8.54 (d, J = 9.2 Hz, 1H), 7.80−7.77 (m, 2H), 7.65−

DOI: 10.1021/acs.jmedchem.6b01066
J. Med. Chem. XXXX, XXX, XXX−XXX

7.58 (m, 1H), 7.54 (m, 2H), 4.48 (dd, J = 9.0, 3.4 Hz, 1H), 4.15 (d, J = 3.9 Hz, 1H). ^{13}C NMR (101 MHz, DMSO-d_6) δ: 168.7, 167.9, 140.6, 133.0, 129.2, 126.9, 55.5, 54.3. LCMS (ES+) m/z 289.0 $[M + H]^+$, $C_{10}H_{13}N_2O_6S$ requires 289.0.

*(2S,3S)-3-(Phenylsulfonamido)aspartic Acid (**4a-B**).* General procedure A. Yield 9 mg, 8%. ^{1}H NMR (400 MHz, DMSO-d_6) δ: 8.66 (br s, 3H), 8.31 (d, J = 9.4 Hz, 1H), 7.84−7.81 (m, 2H), 7.65−7.58 (m, 1H), 7.54 (m, 2H), 4.50 (dd, J = 9.0, 3.7 Hz, 1H), 4.09 (br s, 1H). ^{13}C NMR (101 MHz, DMSO-d_6) δ: 168.0, 167.3, 140.2, 133.1, 129.3, 127.1, 55.8, 54.9. LCMS (ES+) m/z 289.0 $[M + H]^+$, $C_{10}H_{13}N_2O_6S$ requires 289.0.

*(2S)-3-(Naphthalene-1-sulfonamido)aspartic Acid (**4b**).* General procedure A. Yield from **9**: 47 mg, 29%. Diastereomer 1: ^{1}H NMR (600 MHz, DMSO-d_6) δ: 8.74 (dd, J = 8.6, 1.1 Hz, 1H), 8.49 (broad s, 3H), 8.24 (d, J = 8.2 Hz, 1H), 8.20 (dd, J = 7.4, 1.2 Hz, 1H), 8.11−8.05 (m, 1H), 7.72 (dt, J = 8.4, 1.4 Hz, 1H), 7.68−7.66 (m, 1H), 7.63 (t, J = 8.1 Hz, 1H), 4.43 (broad s, 1H), 4.19 (broad s, 1H). Diastereomer 2: ^{1}H NMR (600 MHz, DMSO-d_6) δ: 8.67−8.62 (m, 1H), 8.47 (s, 3H), 8.24 (d, J = 8.2 Hz, 1H), 8.16 (dd, J = 7.3, 1.2 Hz, 1H), 8.08 (m, 1H), 7.74−7.70 (m, 1H), 7.69−7.65 (m, 1H), 7.66−7.62 (m, 1H), 4.45−4.41 (m, 1H), 4.17 (d, J = 4.0 Hz, 1H). Diastereomer 1 (d1) and diastereomer 2 (d2): ^{13}C NMR (151 MHz, DMSO-d_6) δ: 168.4 (d2), 167.7 (d2), 167.7 (d1), 167.1 (d1), 135.0, 134.9, 134.3, 134.3, 133.8, 128.9, 128.8, 128.7, 127.8, 127.8, 127.8, 127.7, 126.8, 126.8, 125.1, 124.8, 124.3, 55.5 (d1), 55.3 (d2), 54.8 (d1), 54.0 (d2). LCMS (ES+) m/z 339.0 $[M + H]^+$, $C_{14}H_{15}N_2O_6S$ requires 339.1.

*(2S)-3-(Naphthalene-2-sulfonamido)aspartic Acid (**4c**).* General procedure A. Yield from **9**: 22 mg, 14%. Diastereomer 1: ^{1}H NMR (600 MHz, DMSO-d_6) δ: 8.51 (s, 3H), 8.43 (d, J = 1.7 Hz, 1H), 8.17−8.13 (m, 1H), 8.12 (d, J = 8.8 Hz, 1H), 8.05 (dt, J = 8.1, 1.6 Hz, 1H), 7.88 (dd, J = 8.7, 1.9 Hz, 1H), 7.73−7.70 (m, 1H), 7.69−7.66 (m, 1H), 4.46−4.43 (m, 1H), 4.24 (d, J = 3.1 Hz, 1H). Diastereomer 2: ^{1}H NMR (600 MHz, DMSO-d_6) δ: 8.51 (s, 3H), 8.45 (d, J = 1.5 Hz, 1H), 8.17−8.13 (m, 1H), 8.11 (d, J = 8.7 Hz, 1H), 8.05 (dt, J = 8.1, 1.6 Hz, 1H), 7.84 (dd, J = 8.7, 1.9 Hz, 1H), 7.73−7.70 (m, 1H), 7.69−7.66 (m, 1H), 4.48 (d, J = 4.1 Hz, 1H), 4.18 (d, J = 4.2 Hz, 1H). Diastereomer 1: ^{13}C NMR (151 MHz, DMSO-d_6) δ: 167.7, 167.2, 137.1, 134.3, 131.5, 129.2, 129.0, 128.8, 127.8, 127.6, 127.5, 122.8, 55.7, 54.5. Diastereomer 2: ^{13}C NMR (151 MHz, DMSO-d_6) δ: 168.5, 167.8, 137.2, 134.3, 131.5, 129.3, 129.1, 128.8, 127.8, 127.6, 127.5, 122.5, 55.4, 54.1. LCMS (ES+) m/z 339.1 $[M + H]^+$, $C_{14}H_{15}N_2O_6S$ requires 339.1.

*(2S)-3-((Perfluorophenyl)sulfonamido)aspartic Acid (**4d-A**).* General procedure A. Yield from **9**: 7.0 mg, 4%. One single diastereomer: ^{1}H NMR (600 MHz, D_2O) δ: 4.74−4.69 (m, 2H). ^{13}C NMR (151 MHz, D_2O) δ: 169.6, 168.6, 145.7, 145.6, 144.0, 143.8, 138.8, 137.2, 114.2, 56.4, 55.1. ^{19}F NMR (376 MHz, D_2O) δ: −136.56 to −136.71 (m), −145.07 (tt, J = 21.1, 7.4 Hz), −159.57 to −159.75 (m). LCMS (ES+) m/z 379.0 $[M + H]^+$, $C_{10}H_8F_5N_2O_6S$ requires 379.0.

*(2S)-3-((Perfluorophenyl)sulfonamido)aspartic Acid (**4d-B**).* General procedure A. Yield from **9**: 4.3 mg, 2%. One single diastereomer: ^{1}H NMR (400 MHz, D_2O) δ: 4.90 (d, J = 3.5 Hz, 1H), 4.58 (d, J = 3.5 Hz, 1H). ^{13}C NMR (151 MHz, D_2O) δ: 169.7, 168.7, 145.6, 145.5, 143.9, 143.8, 138.8, 137.2, 114.5, 55.4, 54.5. ^{19}F NMR (376 MHz, D_2O) δ: −137.13 to −137.28 (m), −145.03 (tt, J = 21.3, 7.5 Hz), −159.56 to −159.74 (m). LCMS (ES+) m/z 379.0 $[M + H]^+$, $C_{10}H_8F_5N_2O_6S$ requires 379.0.

*(2S)-3-((4-Fluorophenyl)sulfonamido)aspartic Acid (**4e**).* General procedure A. Yield from **9**: 44 mg, 30%. Diastereomer 1: ^{1}H NMR (600 MHz, DMSO-d_6) δ: 8.55 (broad s, 3H), 7.94−7.84 (m, 2H), 7.45−7.39 (m, 2H), 4.44−4.36 (m, 1H), 4.22 (dd, J = 3.1 Hz, 1H). Diastereomer 2: ^{1}H NMR (600 MHz, DMSO-d_6) δ: 8.55 (s, 3H), 7.94−7.84 (m, 2H), 7.45−7.39 (m, 2H), 4.44−4.36 (m, 1H), 4.15 (dd, J = 4.2, 1.6 Hz, 1H). Diastereomer 1: ^{13}C NMR (151 MHz, DMSO-d_6) δ: 167.7, 167.2, 165.1, 165.1, 136.5, 136.5, 130.0, 130.0, 116.0, 116.0, 55.7, 54.4. Diastereomer 2: ^{13}C NMR (151 MHz, DMSO-d_6) δ: 168.5, 167.8, 163.5, 163.5, 136.7, 129.9, 129.8, 116.2, 116.2, 55.3, 54.1. ^{19}F NMR (376 MHz, DMSO-d_6) δ: −106.6. LCMS (ES+) m/z 307.0 $[M + H]^+$, $C_{10}H_{12}FN_2O_6S$ requires 307.0.

*(2S)-3-((4-Chlorophenyl)sulfonamido)aspartic Acid (**4f**).* General procedure A. Yield from **9**: 46 mg, 30%. Diastereomer 1: ^{1}H NMR (600 MHz, DMSO-d_6) δ: 8.64 (s, 3H), 7.88−7.79 (m, 2H), 7.69−7.63 (m, 2H), 4.44 (m, 1H), 4.16 (d, J = 4.1 Hz, 1H). Diastereomer 2: ^{1}H NMR (600 MHz, DMSO-d_6) δ: 8.64 (s, 3H), 7.88−7.79 (m, 2H), 7.69−7.63 (m, 2H), 4.41 (broad s, 1H), 4.25−4.21 (m, 1H). Diastereomer 1: ^{13}C NMR (151 MHz, DMSO-d_6) δ: 168.5, 167.8, 139.2, 137.6, 129.1, 128.7, 55.3, 54.1. Diastereomer 2: ^{13}C NMR (151 MHz, DMSO-d_6) δ: 167.7, 167.1, 139.0, 137.6, 129.1, 128.9, 55.7, 54.4. LCMS (ES+) m/z 323.0 $[M + H]^+$, $C_{10}H_{12}ClN_2O_6S$ requires 323.0.

*(2S)-3-((4-Bromophenyl)sulfonamido)aspartic Acid (**4g**).* General procedure B; 10 mol % 4-bromobenzenesulfonate. Yield from **9**: 29 mg, 17%. Diastereomer 1: ^{1}H NMR (400 MHz, D_2O) δ: 7.83 (s, 4H), 4.67 (d, J = 3.1 Hz, 1H), 4.53 (d, J = 3.1 Hz, 1H). Diastereomer 2: ^{1}H NMR (400 MHz, D_2O) δ: 7.83 (s, 4H), 4.53 (d, J = 4.8 Hz, 1H), 4.37 (d, J = 4.3 Hz, 1H). Diastereomer 1 ^{13}C NMR (151 MHz, D_2O) δ: 170.3, 169.5, 137.8, 133.5, 129.6, 129.3, 56.8, 56.0. Diastereomer 2: ^{13}C NMR (151 MHz, D_2O) δ: 171.2, 170.2, 137.9, 133.6, 129.6, 129.3, 56.6, 55.9. LCMS (ES+) m/z 367.0 $[M + H]^+$, 369.0 $[m + 2 + H]^+$, $C_{10}H_{12}BrN_2O_6S$ requires 367.0 and 369.0.

*(2S)-3-((4-Methylphenyl)sulfonamido)aspartic Acid (**4h**).* General procedure A. Yield from **9**: 33 mg, 23%. Diastereomer 1: ^{1}H NMR (600 MHz, DMSO-d_6) δ: 8.35 (br s, 3H), 7.72 (d, J = 8.4 Hz, 2H), 7.40−7.35 (m, 2H), 4.41−4.29 (m, 1H), 4.17−4.12 (m, 1H), 2.38 (s, 3H). Diastereomer 2: ^{1}H NMR (600 MHz, DMSO-d_6) δ: 8.35 (br s, 3H), 7.72 (d, J = 8.4 Hz, 2H), 7.40−7.35 (m, 2H), 4.41−4.29 (m, 1H), 4.11 (d, J = 4.0 Hz, 1H), 2.38 (s, 3H). Diastereomer 1: ^{13}C NMR (151 MHz, DMSO-d_6) δ: 167.7, 167.2, 143.0, 137.1, 129.4, 126.9, 55.7, 54.6, 21.0. Diastereomer 2: ^{13}C NMR (151 MHz, DMSO-d_6) δ: 168.5, 167.9, 143.0, 137.4, 129.4, 126.8, 55.3, 54.1, 21.0. LCMS (ES+) m/z 303.1 $[M + H]^+$, $C_{11}H_{15}N_2O_6S$ requires 303.1.

*(2S)-3-((4-(tert-Butyl)phenyl)sulfonamido)aspartic Acid (**4i**).* General procedure B; 12 mol % 4-*tert*-butylbenzenesulfonate. Yield from **9**: 40 mg, 24%. Diastereomer 1: ^{1}H NMR (400 MHz, D_2O) δ: 7.87 (dd, J = 8.8, 2.4 Hz, 2H), 7.72 (dd, J = 8.8, 2.5 Hz, 2H), 4.65 (d, J = 3.1 Hz, 1H), 4.50 (d, J = 3.1 Hz, 1H), 1.36 (s, 9H). Diastereomer 2: ^{1}H NMR (400 MHz, D_2O) δ: 7.87 (dd, J = 8.8, 2.4 Hz, 2H), 7.72 (dd, J = 8.8, 2.5 Hz, 2H), 4.47 (d, J = 4.5 Hz, 1H), 4.35 (d, J = 4.4 Hz, 1H), 1.36 (s, 9H). Diastereomer 1: ^{13}C NMR (151 MHz, D_2O) δ: 170.3, 169.6, 159.3, 135.4, 127.9, 127.5, 56.8, 56.1, 35.6, 31.1. Diastereomer 2: ^{13}C NMR (151 MHz, D_2O) δ: 171.2, 170.2, 159.4, 135.4, 127.9, 127.5, 56.6, 55.9, 35.6, 31.1. LCMS (ES+) m/z 345.1 $[M + H]^+$, $C_{14}H_{21}N_2O_6S$ requires 345.1.

*(2S)-3-((4-(Methylsulfonyl)phenyl)sulfonamido)aspartic Acid (**4j**).* General procedure B. Yield from **9**: 23 mg, 13%. Diastereomer 1: ^{1}H NMR (400 MHz, DMSO-d_6) δ: 8.16−8.10 (m, 2H), 8.10−8.04 (m, 2H), 4.52−4.45 (m, 1H), 4.22 (d, J = 4.1 Hz, 1H), 3.29 (s, 3H). Diastereomer 2: ^{1}H NMR (400 MHz, DMSO-d_6) δ: 8.16−8.10 (m, 2H), 8.10−8.04 (m, 2H), 4.52−4.45 (m, 1H), 4.35−4.28 (m, 1H), 3.29 (s, 3H). Diastereomer 1: ^{13}C NMR (151 MHz, DMSO-d_6) δ: 167.6, 166.9, 144.7, 144.2, 128.0, 127.8, 55.2, 54.2, 43.2. Diastereomer 2: ^{13}C NMR (151 MHz, DMSO-d_6) δ: 168.3, 167.6, 144.9, 144.2, 127.8, 127.7, 55.7, 53.8, 43.2. LCMS (ES+) m/z 367.1 $[M + H]^+$, $C_{11}H_{15}N_2O_8S_2$ requires 367.0.

*(2S)-3-((4-Methoxyphenyl)sulfonamido)aspartic Acid (**4k**).* General procedure A. Yield from **9**: 43 mg, 28%. Diastereomer 1: ^{1}H NMR (600 MHz, D_2O) δ: 7.81 (dd, J = 8.9, 3.0 Hz, 2H), 7.07 (dd, J = 9.1, 3.1 Hz, 2H), 4.73 (d, J = 3.1 Hz, 1H), 4.52 (d, J = 3.1 Hz, 1H), 3.85 (s, 3H). Diastereomer 2: ^{1}H NMR (600 MHz, D_2O) δ: 7.81 (dd, J = 9.0, 3.1 Hz, 2H), 7.07 (dd, J = 9.1, 3.0 Hz, 2H), 4.55 (d, J = 4.1 Hz, 1H), 4.45 (d, J = 4.1 Hz, 1H), 3.86 (s, 3H). Diastereomer 1: ^{13}C NMR (151 MHz, D_2O) δ: 170.3, 169.3, 164.2, 130.4, 130.2, 115.6, 56.7, 56.6, 55.9. Diastereomer 2: ^{13}C NMR (151 MHz, D_2O) δ: 171.2, 170.0, 164.3, 130.4, 130.2, 115.6, 56.7, 56.4, 55.7. LCMS (ES+) m/z 319.1 $[M + H]^+$, $C_{11}H_{15}N_2O_7S$ requires 319.1.

*(2S)-3-((4-(Trifluoromethyl)phenyl)sulfonamido)aspartic Acid (**4l**).* General procedure B. Yield from **9**: 52 mg, 31%. Diastereomer 1: ^{1}H NMR (400 MHz, D_2O) δ: 8.10 (d, J = 8.2 Hz, 2H), 7.97 (d, J = 8.8 Hz, 2H), 4.67 (d, J = 4.1 Hz, 1H), 4.48 (d, J = 4.1 Hz, 1H).

DOI: 10.1021/acs.jmedchem.6b01066
J. Med. Chem. XXXX, XXX, XXX−XXX

Diastereomer 2: ^{1}H NMR (400 MHz, D_2O) δ: 8.10 (d, J = 8.2 Hz, 2H), 7.96 (d, J = 8.7 Hz, 2H), 4.76 (m, inter alia 1H), 4.63 (d, J = 3.1 Hz, 1H). Diastereomer 1: ^{13}C NMR (151 MHz, D_2O) δ: 170.8, 169.9, 142.6, 135.5, 135.3, 128.7, 127.6, 127.5, 126.9, 125.1, 123.3, 121.5, 56.3, 55.7. Diastereomer 2: ^{13}C NMR (151 MHz, D_2O) δ: 170.0, 169.1, 142.4, 135.5, 135.2, 128.7, 127.5, 127.5, 126.9, 125.1, 123.3, 121.5, 56.7, 55.7. ^{19}F NMR (376 MHz, D_2O) δ: −63.1. LCMS (ES+) m/z 357.0 $[M + H]^+$, $C_{11}H_{12}F_3N_2O_6S$ requires 357.0.

*(2S)-3-((4-Nitrophenyl)sulfonamido)aspartic Acid (**4m**).* General procedure B. Yield from **9**: 32 mg, 20%. Diastereomer 1: ^{1}H NMR (400 MHz, D_2O) δ: 8.48−8.39 (m, 2H), 8.19−8.12 (m, 2H), 4.79 (m, inter alia 1H), 4.66 (d, J = 3.1 Hz, 1H). Diastereomer 2: ^{1}H NMR (400 MHz, D_2O) δ: 8.44 (d, J = 9.0 Hz, 2H), 8.15 (d, J = 8.9 Hz, 2H), 4.71 (d, J = 3.9 Hz, 1H), 4.50 (d, J = 3.9 Hz, 1H). Diastereomer 1: ^{13}C NMR (151 MHz, D_2O) δ: 170.0, 169.0, 151.4, 144.7, 129.5, 125.5, 56.7, 55.6. Diastereomer 2: ^{13}C NMR (151 MHz, D_2O) δ: 170.8, 169.8, 151.4, 144.8, 129.5, 125.6, 56.3, 55.6. LCMS (ES+) m/z 334.1 $[M + H]^+$, $C_{10}H_{12}N_3O_8S$ requires 334.0.

*(2S)-3-((4-Aminophenyl)sulfonamido)aspartic Acid (**4n**).* General procedure A; 18 mol % triethylammonium chloride. Yield from **9** (150 mg, 0.358 mmol): 29 mg, 26%. Diastereomer 1: ^{1}H NMR (600 MHz, D_2O) δ: 8.03−8.01 (m, 2H), 7.59−7.56 (m, 2H), 4.76 (d, J = 3.1 Hz, 1H), 4.61 (d, J = 3.1 Hz, 1H). Diastereomer 2: ^{1}H NMR (600 MHz, D_2O) δ: 8.02−8.00 (m, 2H), 7.59−7.56 (m, 2H), 4.66 (d, J = 4.0 Hz, 1H), 4.49 (d, J = 3.9 Hz, 1H). Diastereomer 1: ^{13}C NMR (151 MHz, D_2O) δ: 170.0, 168.9, 139.0, 136.7, 130.1, 124.7, 56.5, 55.6. Diastereomer 2: ^{13}C NMR (151 MHz, D_2O) δ: 170.7, 169.7, 139.0, 136.9, 130.1, 124.7, 56.2, 55.5. LCMS (ES+) m/z 303.9 $[M + H]^+$, $C_{10}H_{14}N_3O_6S$ requires 304.1.

*(3S)-2-((4-Acetylphenyl)sulfonamido)-3-aminoaspartic Acid (**4o**).* General procedure A. Yield from **9** (150 mg, 0.358 mmol): 6.5 mg, 6%. Diastereomer 1: ^{1}H NMR (600 MHz, D_2O) δ: 8.17−8.14 (m, 2H), 8.05−8.02 (m, 2H), 4.78−4.77 (m, inter alia 1H), 4.63 (d, J = 3.1 Hz, 1H), 2.71 (s, 3H). Diastereomer 2: ^{1}H NMR (600 MHz, D_2O) δ: 8.17−8.14 (m, 2H), 8.05−8.02 (m, 2H), 4.69 (d, J = 4.1 Hz, 1H), 4.50 (d, J = 4.1 Hz, 1H), 2.71 (s, 3H). Diastereomer 1: ^{13}C NMR (151 MHz, D_2O) δ: 203.3, 169.9, 169.0, 142.9, 141.2, 130.2, 128.4, 56.6, 55.7, 27.5. Diastereomer 2: ^{13}C NMR (151 MHz, D_2O) δ: 203.3, 170.7, 169.7, 143.1, 141.3, 130.3, 128.4, 56.2, 55.6, 27.5. LCMS (ES+) m/z 330.8 $[M + H]^+$, $C_{12}H_{15}N_2O_7S$ requires 331.0.

*(3S)-2-([1,1′-Biphenyl]-4-sulfonamido)-3-aminoaspartic Acid (**4p**).* General procedure B; 6 mol % triethylammonium chloride. Yield from **9** (150 mg, 0.358 mmol): 25 mg, 19%. Diastereomer 1: ^{1}H NMR (600 MHz, methanol-d_4/MeCN-d_3 1:1) δ: 8.00 (d, J = 8.5 Hz, 2H), 7.82 (d, J = 8.4 Hz, 2H), 7.71−7.67 (m, 2H), 7.49 (t, J = 7.7 Hz, 2H), 7.43 (t, J = 7.3 Hz, 1H), 4.59 (d, J = 2.9 Hz, 1H), 4.44 (d, J = 2.8 Hz, 1H). Diastereomer 2: ^{1}H NMR (600 MHz, methanol-d_4/MeCN-d_3 1:1) δ: 7.98 (d, J = 8.4 Hz, 2H), 7.83 (d, J = 8.3 Hz, 2H), 7.71−7.67 (m, 2H), 7.49 (t, J = 7.7 Hz, 2H), 7.43 (t, J = 7.3 Hz, 1H), 4.54 (d, J = 4.1 Hz, 1H), 4.34 (d, J = 4.1 Hz, 1H). Diastereomer 1: ^{13}C NMR (151 MHz, methanol-d_4/MeCN-d_3 1:1) δ: 168.9, 168.1, 147.2, 140.5, 139.2, 130.2, 129.7, 129.2, 128.6, 128.3, 57.0, 56.2. Diastereomer 2: ^{13}C NMR (151 MHz, methanol-d_4/MeCN-d_3 1:1) δ: 170.1, 168.8, 147.2, 140.5, 139.5, 130.2, 129.7, 129.1, 128.6, 128.3, 56.6, 55.9. LCMS (ES+) m/z 364.9 $[M + H]^+$, $C_{16}H_{17}N_2O_6S$ requires 365.1.

*(2S)-3-((3-Chlorophenyl)sulfonamido)aspartic Acid (**4q**).* General procedure A. Yield from **9**: 41 mg, 27%. Diastereomer 1: ^{1}H NMR (600 MHz, DMSO-d_6) δ: 8.69 (s, 3H), 7.85 (t, J = 1.9 Hz, 1H), 7.73 (ddt, J = 8.1, 2.2, 1.1 Hz, 2H), 7.61 (t, J = 8.0 Hz, 1H), 4.45 (d, J = 4.1 Hz, 1H), 4.14 (d, J = 4.0 Hz, 1H). Diastereomer 2: ^{1}H NMR (600 MHz, DMSO-d_6) δ: 8.69 (s, 3H), 7.88 (t, J = 1.9 Hz, 1H), 7.77 (ddt, J = 7.8, 2.7, 1.2 Hz, 2H), 7.61 (t, J = 8.0 Hz, 1H), 4.41 (d, J = 2.9 Hz, 1H), 4.25 (d, J = 3.0 Hz, 1H). Diastereomer 1: ^{13}C NMR (151 MHz, DMSO-d_6) δ: 168.5, 167.9, 142.2, 133.5, 132.6, 130.9, 126.5, 125.4, 55.4, 54.1. Diastereomer 2: ^{13}C NMR (151 MHz, DMSO-d_6) δ: 167.7, 167.2, 142.0, 133.5, 132.6, 131.0, 126.7, 125.5, 55.9, 54.4. LCMS (ES+) m/z 323.0 $[M + H]^+$, $C_{10}H_{12}ClN_2O_6S$ requires 323.0.

*(2S)-3-((3-(Trifluoromethyl)phenyl)sulfonamido)aspartic Acid (**4r**).* General procedure B. Yield from **9**: 27 mg, 16%. Diastereomer 1: ^{1}H NMR (600 MHz, DMSO-d_6) δ: 8.74 (s, 3H), 8.17 (d, J = 1.8 Hz, 1H), 8.13−8.09 (m, 1H), 8.04 (dd, J = 8.0, 2.1 Hz, 1H), 7.83 (td, J = 7.9, 2.4 Hz, 1H), 4.42 (d, J = 4.0 Hz, 1H), 4.29−4.25 (m, 1H). Diastereomer 2: ^{1}H NMR (600 MHz, DMSO-d_6) δ: 8.74 (s, 3H), 8.13 (d, J = 1.7 Hz, 1H), 8.13−8.09 (m, 1H), 8.04 (dd, J = 8.0, 2.1 Hz, 1H), 7.83 (td, J = 7.9, 2.4 Hz, 1H), 4.48 (m, 1H), 4.15 (d, J = 4.0 Hz, 1H). Diastereomer 1: ^{13}C NMR (151 MHz, DMSO-d_6) δ: 167.7, 167.2, 141.3, 130.8, 130.4, 129.9, 129.6, 129.4, 129.4, 129.2, 126.2, 124.4, 123.9, 123.8, 123.8, 123.8, 122.6, 120.8, 55.9, 54.3. Diastereomer 2: ^{13}C NMR (151 MHz, DMSO-d_6) δ: 168.5, 168.0, 167.7, 167.2, 141.6, 130.8, 130.5, 129.9, 129.7, 129.4, 129.4, 129.4, 129.2, 126.2, 124.4, 123.6, 123.6, 123.5, 123.5, 122.6, 120.8, 55.4, 54.1. Diastereomer 1: ^{19}F NMR (376 MHz, DMSO-d_6) δ: −61.36 (d, J = 1.4 Hz). Diastereomer 2: ^{19}F NMR (376 MHz, DMSO-d_6) δ: −61.34 (d, J = 1.3 Hz). LCMS (ES+) m/z 357.0 $[M + H]^+$, $C_{11}H_{12}F_3N_2O_6S$ requires 357.0.

*(2S)-3-((3-Carboxyphenyl)sulfonamido)aspartic Acid (**4s**).* Using a modified general procedure A, **9** (125 mg, 0.30 mmol) was dissolved in dry CH_2Cl_2 (3 mL) under argon gas. Triethylamine (125 μL, 0.90 mmol) was added, and after 5 min of stirring, 3-cyanobenzenesulfonyl chloride (91 mg, 0.45 mmol) was added. The reaction mixture was stirred overnight and evaporated. Without further purification, the crude was treated with 6 M HCl (11.5 mL) and stirred in a closed vial overnight at 110 °C. The reaction mixture was washed with Et_2O (3 × 3 mL) and CH_2Cl_2 (3 × 3 mL). The solvent was evaporated and purified by preparative HPLC to yield (2*S*)-3-((3-carboxyphenyl)-sulfonamido)aspartic acid (19 mg, 0.06 mmol, 19%). Diastereomer 1: ^{1}H NMR (400 MHz, D_2O) δ: 8.47 (t, J = 1.8 Hz, 1H), 8.29 (dt, J = 7.9, 1.4 Hz, 1H), 8.15 (ddd, J = 8.0, 2.0, 1.1 Hz, 1H), 7.74 (t, J = 7.9 Hz, 1H), 4.76 (d, J = 3.1 Hz, 1H), 4.61 (d, J = 3.1 Hz, 1H). Diastereomer 2: ^{1}H NMR (400 MHz, D_2O) δ: 8.48 (t, J = 1.8 Hz, 1H), 8.30 (dt, J = 7.8, 1.4 Hz, 1H), 8.15 (ddd, J = 8.0, 2.0, 1.1 Hz, 1H), 7.75 (t, J = 7.9 Hz, 1H), 4.62 (d, J = 4.2 Hz, 1H), 4.44 (d, J = 4.2 Hz, 1H). LCMS (ES+) m/z 333.1 $[M + H]^+$, $C_{11}H_{13}N_2O_8S$ requires 333.0.

*(2S)-3-((2-Chlorophenyl)sulfonamido)aspartic Acid (**4t**).* General procedure A. Yield from **9**: 59 mg, 38%. Diastereomer 1: ^{1}H NMR (600 MHz, DMSO-d_6) δ: 8.47 (broad s, 3H), 7.98−7.93 (m, 1H), 7.68−7.63 (m, 2H), 7.56−7.50 (m, 1H), 4.49 (d, J = 3.9 Hz, 1H), 4.30 (d, J = 4.0 Hz, 1H). Diastereomer 2: ^{1}H NMR (600 MHz, DMSO-d_6) δ: 8.47 (broad s, 3H), 8.02 (dd, J = 7.5, 1.3 Hz, 1H, 7.68−7.63 (m, 2H), 7.56−7.50 (m, 1H), 4.60 (d, J = 3.1 Hz, 1H), 4.22 (d, J = 3.2 Hz, 1H). Diastereomer 1: ^{13}C NMR (151 MHz, DMSO-d_6) δ: 168.3, 167.8, 137.4, 134.3, 131.6, 131.2, 130.2, 127.5, 55.6, 53.9. Diastereomer 2: ^{13}C NMR (151 MHz, DMSO-d_6) δ: 168.1, 167.2, 137.6, 134.3, 131.7, 131.1, 130.4, 127.5, 55.9, 55.0. LCMS (ES+) m/z 323.0 $[M + H]^+$, $C_{10}H_{12}ClN_2O_6S$ requires 323.0.

*(2S)-3-((2-Methylphenyl)sulfonamido)aspartic Acid (**4u**).* General procedure A. Yield from **9** (250 mg, 0.597 mmol): 38 mg, 21%. Diastereomer 1: ^{1}H NMR (600 MHz, D_2O) δ: 7.92 (dd, J = 7.9, 1.0 Hz, 1H), 7.59−7.53 (m, 1H), 7.41 (d, J = 8.2 Hz, 1H), 7.40−7.34 (m, 1H), 4.70 (d, J = 3.2 Hz, 1H), 4.44 (d, J = 3.3 Hz, 1H), 2.64 (s, 3H). Diastereomer 2: ^{1}H NMR (600 MHz, D_2O) δ: 7.91 (dd, J = 8.0, 1.0 Hz, 1H), 7.59−7.55 (m, 1H), 7.42 (d, J = 7.7 Hz, 1H), 7.40−7.36 (m, 1H), 4.49 (d, J = 4.2 Hz, 1H), 4.43 (d, J = 4.2 Hz, 1H), 2.59 (s, 3H). Diastereomer 1: ^{13}C NMR (151 MHz, D_2O) δ: 170.1, 169.0, 139.1, 136.0, 135.0, 133.8, 130.4, 127.2, 56.2, 55.7, 20.5. Diastereomer 2: ^{13}C NMR (151 MHz, D_2O) δ: 170.9, 169.6, 138.8, 136.2, 135.1, 133.8, 130.4, 127.3, 55.9, 55.3, 20.3. LCMS (ES+) m/z 303.1 $[M + H]^+$, $C_{11}H_{15}N_2O_6S$ requires 303.1.

*(2S)-3-((3,5-Dimethylphenyl)sulfonamido)aspartic Acid (**4v**).* General procedure A. Yield from **9**: 23 mg, 15%. Diastereomer 1: ^{1}H NMR (600 MHz, DMSO-d_6) δ: 8.33 (broad s, 3H), 7.43−7.41 (m, 2H), 7.30−7.26 (m, 1H), 4.35−4.30 (m, 1H), 4.08 (d, J = 4.3 Hz, 1H), 2.34 (s, 6H). Diastereomer 2: ^{1}H NMR (600 MHz, DMSO-d_6) δ: 8.33 (br s, 3H), 7.55−7.43 (m, 2H), 7.30−7.26 (m, 1H), 4.29 (br s, 1H), 4.17 (br s, 1H), 2.34 (s, 6H). Diastereomer 1: ^{13}C NMR (151 MHz, DMSO-d_6) δ: 168.5, 167.9, 139.9, 138.4, 134.1, 124.2, 55.3, 54.1, 20.7. Diastereomer 2: ^{13}C NMR (151 MHz, DMSO-d_6) δ: 167.7, 167.2, 139.7, 138.4, 134.1, 124.4, 55.8, 54.6, 20.7. LCMS (ES+) m/z 317.1 $[M + H]^+$, $C_{12}H_{17}N_2O_6S$ requires 317.1.

*(2S)-3-((2,6-Dichlorophenyl)sulfonamido)aspartic Acid (**4x**).* General procedure B. Yield from **9**: 52 mg, 30%. Diastereomer 1: ^{1}H NMR

DOI: 10.1021/acs.jmedchem.6b01066
J. Med. Chem. XXXX, XXX, XXX−XXX

(600 MHz, D_2O) δ: 7.62−7.59 (m, 2H), 7.54−7.50 (m, 1H), 4.70 (d, J = 3.5 Hz, 1H), 4.69 (d, J = 3.4 Hz, 1H). Diastereomer 2: ^{1}H NMR (600 MHz, D_2O) δ: 7.62−7.59 (m, 2H), 7.54−7.50 (m, 1H), 4.71 (d, J = 4.4 Hz, 1H), 4.49 (d, J = 4.4 Hz, 1H). Diastereomer 1: ^{13}C NMR (151 MHz, D_2O) δ: 170.2, 169.1, 135.4, 135.0, 133.7, 132.5, 56.7, 55.7. Diastereomer 2: ^{13}C NMR (151 MHz, D_2O) δ: 170.8, 169.6, 135.3, 134.9, 134.0, 132.5, 56.4, 55.2. LCMS (ES+) m/z 357.0 $[M + H]^+$, $C_{10}H_{11}Cl_2N_2O_6S$ requires 357.0.

*(2S)-3-((3,4-Difluorophenyl)sulfonamido)aspartic Acid (**4y**).* General procedure B. Yield from **9**: 45 mg, 29%. Diastereomer 1: ^{1}H NMR (400 MHz, D_2O) δ: 7.93−7.86 (m, 1H), 7.81−7.76 (m, 1H), 7.57−7.49 (m, 1H), 4.70 (d, J = 3.1 Hz, 1H), 4.56 (d, J = 3.1 Hz, 1H). Diastereomer 2: ^{1}H NMR (400 MHz, D_2O) δ: 7.93−7.86 (m, 1H), 7.81−7.76 (m, 1H), 7.57−7.49 (m, 1H), 4.58 (d, J = 4.2 Hz, 1H), 4.41 (d, J = 4.2 Hz, 1H). Diastereomer 1: ^{13}C NMR (151 MHz, D_2O) δ: 170.3, 169.4, 155.3, 155.3, 153.5, 153.5, 151.6, 150.1, 135.6, 135.6, 135.6, 135.6, 125.8, 125.8, 125.7, 119.6, 119.5, 118.1, 118.0, 56.8, 55.9. Diastereomer 2: ^{13}C NMR (151 MHz, D_2O) δ: 171.2, 170.1, 155.2, 155.2, 153.6, 153.6, 151.7, 150.0, 135.7, 135.7, 135.7, 135.7, 125.8, 125.8, 125.8, 119.6, 119.5, 118.1, 118.0, 56.6, 55.9. Diastereomer 1: ^{19}F NMR (376 MHz, D_2O) δ: −129.36 (d, J = 20.6 Hz), −134.74 (d, J = 20.9 Hz). Diastereomer 2: ^{19}F NMR (376 MHz, D_2O) δ: −129.23 (d, J = 20.9 Hz), −134.64 (d, J = 20.4 Hz). LCMS (ES+) m/z 325.0 $[M + H]^+$, $C_{10}H_{11}F_2N_2O_6S$ requires 325.0.

*(2S)-3-((2,4,5-Trifluorophenyl)sulfonamido)aspartic Acid (**4z**).* General procedure A. Yield from **9** (150 mg, 0.358 mmol): 48 mg, 39%. Diastereomer 1: ^{1}H NMR (400 MHz, D_2O) δ: 7.77−7.68 (m, 1H), 7.32−7.21 (m, 1H), 4.69 (d, J = 3.7 Hz, 1H), 4.47 (d, J = 3.6 Hz, 1H). Diastereomer 2: ^{1}H NMR (400 MHz, D_2O) δ: 7.77−7.68 (m, 1H), 7.32−7.21 (m, 1H), 4.72 (d, J = 3.1 Hz, 1H), 4.60 (d, J = 3.1 Hz, 1H). Diastereomer 1: ^{13}C NMR (151 MHz, D_2O) δ: 170.6, 169.4, 156.8, 156.7, 156.7, 155.5, 155.1, 155.1, 155.0, 153.8, 147.8, 147.7, 146.2, 146.1, 123.5, 123.4, 119.5, 119.4, 108.8, 108.7, 108.5, 56.0, 55.4. Diastereomer 2: ^{13}C NMR (151 MHz, D_2O) δ: 169.9, 168.6, 156.8, 156.8, 156.7, 155.5, 155.1, 155.1, 155.0, 153.8, 147.8, 147.7, 146.2, 146.1, 123.3, 123.2, 119.6, 119.4, 108.9, 108.7, 108.5, 56.6, 55.3. Diastereomer 1: ^{19}F NMR (376 MHz, D_2O) δ: −110.08 (dd, J = 15.1, 9.4 Hz), −123.54 (dd, J = 21.4, 9.6 Hz), −140.33 (t, J = 15.2 Hz). Diastereomer 2: ^{19}F NMR (376 MHz, D_2O) δ: −109.38 (dd, J = 15.1, 9.4 Hz), −123.63 (dd, J = 21.3, 9.5 Hz), −140.39 (t, J = 15.1 Hz). LCMS (ES+) m/z 343.0 $[M + H]^+$, $C_{10}H_{10}F_3N_2O_6S$ requires 343.0.

*(2S)-3-((Phenylmethyl)sulfonamido)aspartic Acid (**4aa**).* General procedure B; 9 mol % phenylmethanesulfonate. Yield from **9** (150 mg, 0.358 mmol): 22 mg, 20%. Diastereomer 1: ^{1}H NMR (600 MHz, D_2O) δ: 7.51−7.45 (m, 5H), 4.61 (d, J = 3.5 Hz, inter alia 1H), 4.63−4.56 (m, 2H), 4.28 (d, J = 3.3 Hz, 1H). Diastereomer 2: ^{1}H NMR (600 MHz, D_2O) δ: 7.51−7.45 (m, 5H), 4.65 (d, J = 2.9 Hz, 1H), 4.63−4.56 (m, 2H), 4.53 (d, J = 2.9 Hz, 1H). Diastereomer 1: ^{13}C NMR (151 MHz, D_2O) δ: 170.1, 169.2, 131.9, 130.1, 129.9, 129.0, 60.0, 56.6, 55.9. Diastereomer 2: ^{13}C NMR (151 MHz, D_2O) δ: 171.6, 170.8, 131.9, 130.1, 129.9, 128.9, 59.8, 57.2, 56.3. LCMS (ES+) m/z 302.9 $[M + H]^+$, $C_{11}H_{15}N_2O_6S$ requires 303.1.

*(2S)-3-(Pyridine-3-sulfonamido)aspartic Acid (**4ab**).* General procedure A. Yield from **9** (150 mg, 0.358 mmol): 25 mg, 24%. Diastereomer 1: ^{1}H NMR (600 MHz, D_2O) δ: 9.33 (d, J = 2.0 Hz, 1H), 9.04 (dd, J = 5.8, 1.5 Hz, 1H), 8.98 (dt, J = 8.2, 1.8 Hz, 1H), 8.24 (dd, J = 8.3, 5.7 Hz, 1H), 4.82 (d, J = 3.1 Hz, 1H), 4.73 (d, J = 3.0 Hz, 1H). Diastereomer 2: ^{1}H NMR (600 MHz, D_2O) δ: 9.33 (d, J = 2.0 Hz, 1H), 9.04 (dd, J = 5.8, 1.5 Hz, 1H), 8.98 (dt, J = 8.2, 1.8 Hz, 1H), 8.24 (dd, J = 8.3, 5.7 Hz, 1H), 4.84 (d, J = 3.4 Hz, 1H), 4.54 (d, J = 3.4 Hz, 1H). Diastereomer 1: ^{13}C NMR (151 MHz, D_2O) δ: 169.2, 168.0, 146.3, 144.1, 141.6, 139.0, 127.9, 56.0, 54.5. Diastereomer 2: ^{13}C NMR (151 MHz, D_2O) δ: 170.0, 169.0, 146.3, 144.0, 141.6, 139.3, 127.9, 55.4, 54.7. LCMS (ES+) m/z 289.9 $[M + H]^+$, $C_9H_{12}N_3O_6S$ requires 290.0.

*(2S)-3-(Thiophene-2-sulfonamido)aspartic Acid (**4ac**).* General procedure A. Yield from **9** (150 mg, 0.358 mmol): 14 mg, 13%. Diastereomer 1: ^{1}H NMR (600 MHz, D_2O) δ: 7.90 (dd, J = 5.0, 1.1 Hz, 1H), 7.80−7.75 (m, 1H), 7.23−7.21 (m, 1H), 4.64 (d, J = 4.2 Hz, 1H), 4.45 (d, J = 4.1 Hz, 1H). Diastereomer 2: ^{1}H NMR (600 MHz, D_2O) δ: 7.88 (dd, J = 5.0, 1.1 Hz, 1H), 7.80−7.75 (m, 1H), 7.23−7.21 (m, 1H), 4.74 (d, J = 3.1 Hz, 1H), 4.63 (d, J = 3.1 Hz, 1H). Diastereomer 1: ^{13}C NMR (151 MHz, D_2O) δ: 171.0, 169.9, 138.6, 135.4, 135.0, 129.0, 56.6, 55.7. Diastereomer 2: ^{13}C NMR (151 MHz, D_2O) δ: 170.2, 169.2, 138.6, 135.2, 134.7, 129.1, 56.9, 55.8. LCMS (ES+) m/z 294.8 $[M + H]^+$, $C_8H_{11}N_2O_6S_2$ requires 295.0.

*(2S)-3-(N-Methylphenylsulfonamido)aspartic Acid (**4ad**).* Amine **9** (80 mg, 0.191 mmol) was dissolved in anhyd DCM (2.4 mL) and added TEA (40 μL, 0.287 mmol), followed by phenyl sulfonyl chloride (37 μL, 0.287 mmol) and stirred 20 h. Reaction mixture was subsequently diluted with DCM, washed with 1 M HCl, satd $NaHCO_3$, and then brine. The organic partition was dried over $MgSO_4$, filtered, and concentrated. The crude was dissolved in anhyd DMF (0.46 mL), cooled to 0 °C and K_2CO_3 (78 mg, 0.573 mmol) added, followed by dropwise addition of methyl iodide (50 μL, 3.82 M, 0.191 mmol). Reaction was stirred for 3 h at 0 °C, and an additional equivalent of methyl iodide was added. Reaction was diluted with H_2O and EtOAc, washed four times with H_2O and brine, and dried over $MgSO_4$, followed by filtration and evaporated. Crude was refluxed in 6 M HCl (3 mL) for 4 h, cooled and washed four times with Et_2O and evaporated. Desired compound **4ad** was isolated by purification on preparative HPLC to yield (5.1 mg, 9%). Diastereomer 1: ^{1}H NMR (600 MHz, D_2O) δ: 7.94−7.92 (m, 2H), 7.79−7.74 (m, 1H), 7.69−7.64 (m, 2H), 5.04 (d, J = 8.3 Hz, 1H), 4.54 (d, J = 8.3 Hz, 1H), 2.94 (s, 3H). Diastereomer 2: ^{1}H NMR (600 MHz, D_2O) δ: 7.94−7.92 (m, 2H), 7.79−7.74 (m, 1H), 7.69−7.64 (m, 2H), 5.22 (d, J = 5.8 Hz, 1H), 4.68 (d, J = 5.8 Hz, 1H), 2.94 (s, 3H). Diastereomer 1: ^{13}C NMR (151 MHz, D_2O) δ: 169.9, 169.5, 136.6, 135.2, 130.3, 128.7, 60.6, 53.4, 33.3. Diastereomer 2: ^{13}C NMR (151 MHz, D_2O) δ: 170.2, 169.9, 137.1, 135.0, 130.3, 128.3, 60.4, 54.1, 33.0. LCMS (ES+) m/z 302.9 $[M + H]^+$, $C_{11}H_{15}N_2O_6S$ requires 303.1.

*Dimethyl (2S)-3-Bromo-N-(triphenylmethyl)aspartate (**7**).* Following the optimized procedure for the synthesis, dimethyl (2*S*)-*N*-(triphenylmethyl)aspartate (**6**) (1.00 g, 2.48 mmol) was charged to a flame-dried, argon-purged 100 mL round-bottom flask fitted with septum and dissolved in anhydrous THF (40 mL) at ambient temperature, under argon. Once dissolved, the flask was wrapped in tin foil and cooled to −30 °C for 10 min. Lithium hexamethyldisilazide (2.7 mL 1 M in THF, 2.73 mmol) was added over 30 s, and the resulting mixture was stirred at −30 °C for 30 min. *N*-Bromosuccinimide (500 mg, 2.73 mmol) was added in one portion swiftly to the reaction mixture, which was then allowed to warm to −5 °C over the course of 40 min and maintained at −5 °C for an additional hour. The reaction was quenched by the addition of 15 mL of satd NH_4Cl, warmed to rt, and concentrated in vacuo. The mixture was extracted twice with EtOAc, the combined organic phases were washed with H_2O and brine, dried over $MgSO_4$, filtered, and concentrated in vacuo, yielding a brownish oil (diastereomeric ratio 2:3, conversion by NMR), which was used without further purification due to instability. Diastereomer 1: ^{1}H NMR (600 MHz, chloroform-*d*) δ: 7.50−7.47 (m, 6H), 7.30−7.27 (m, 6H), 7.22−7.18 (m, 3H), 4.25 (d, J = 4.1 Hz, 1H), 3.93 (dd, J = 10.3, 4.2 Hz, 1H), 3.78 (s, 3H), 3.33 (s, 3H), 3.27 (d, J = 10.4 Hz, 1H). Diastereomer 2: ^{1}H NMR (600 MHz, chloroform-*d*) δ: 7.47−7.45 (m, 6H), 7.29−7.27 (m, 6H), 7.22−7.18 (m, 3H), 4.24 (d, J = 6.2 Hz, 1H), 4.10 (dd, J = 10.5, 6.2 Hz, 1H), 3.74 (s, 3H), 3.31 (s, 3H), 3.06 (d, J = 10.5 Hz, 1H).

*Dimethyl (2S)-3-Azido-N-(triphenylmethyl)aspartate (**8**).* Crude dimethyl (2*S*)-3-bromo-*N*-(triphenylmethyl)aspartate (**7**) (theoretically 7.62 mmol) was dissolved in anhydrous DMF (33 mL) under an argon atmosphere in a tin foil covered flask, and NaN_3 (536 mg, 11,43 mmol) was added in one portion. The solution was stirred for 16 h at rt, then diluted with EtOAc and washed with H_2O until a clear organic phase was obtained (4−5 times). The organic phase was washed with brine, dried over $MgSO_4$, filtered, and concentrated. The resulting crude could be used without purification or purified by flash column chromatography (heptane/EtOAc 8:1, 2% TEA) to give **8** as a white, sticky, amorphous syrup (1,90 g, 56% over two steps corrected yield as the amorphous nature of the compound inseparably trapped heptane, diastereomeric ratio 1:1.6). IR (neat): 2113, 1743, 1208, 707 cm^{-1}. Diastereomer 1: ^{1}H NMR (600 MHz, chloroform-*d*) δ: 7.50−7.46 (m,

DOI: 10.1021/acs.jmedchem.6b01066
J. Med. Chem. XXXX, XXX, XXX−XXX

6H), 7.31−7.27 (m, 6H), 7.24−7.17 (m, 3H), 4.04 (dd, J = 8.2, 4.2 Hz, 1H), 3.72 (s, 3H), 3.71 (d, J = 4.3 Hz, 1H), 3.39 (s, 3H), 3.19 (d, J = 8.9 Hz, 1H). Diastereomer 2: ^{1}H NMR (600 MHz, chloroform-d) δ: 7.50−7.46 (m, 6H), 7.31−7.26 (m, 6H), 7.23−7.15 (m, 3H), 3.90 (dd, J = 10.9, 3.2 Hz, 1H), 3.82 (d, J = 3.4 Hz, 1H), 3.78 (s, 3H), 3.26 (s, 3H), 3.11 (d, J = 11.0 Hz, 1H). Diastereomer 1: ^{13}C NMR (151 MHz, $CDCl_3$) δ: 170.9, 168.4, 145.4, 128.9, 128.3, 127.0, 71.5, 65.7, 59.0, 52.8, 52.6. Diastereomer 2: ^{13}C NMR (151 MHz, $CDCl_3$) δ: 171.5, 168.9, 145.3, 128.9, 128.1, 126.8, 71.3, 64.4, 59.2, 53.0, 52.5.

*Dimethyl (2S)-3-Amino-N-(triphenylmethyl)aspartate (**9**).* Dimethyl (2*S*)-3-azido-*N*-(triphenylmethyl)aspartate (**8**) (2.47 g, 5.56 mmol) was dissolved in 66 mL of anhydrous THF in an argon-filled flask. Triphenylphosphine (2.19 g, 8.34 mmol) was added in one portion, followed by the addition of H_2O (150 μL, 8.34 mmol), and the slowly effervescing solution was allowed to stir at ambient temperature for 18 h. The reaction mixture was concentrated in vacuo and purified by flash column chromatography (heptane/EtOAc 8:1 to 4:1 with 5% TEA) to yield **9** as a viscous syrup (1.83 g, 79%, 1:1.7 diastereomeric ratio). The product was immediately stored at −18 °C due to instability. Diastereomer 1: ^{1}H NMR (600 MHz, $CDCl_3$) δ: 7.52−7.49 (m, 6H), 7.29−7.23 (m, 6H), 7.21−7.15 (m, 3H), 3.82 (dd, J = 9.8, 4.4 Hz, 1H), 3.65 (s, 3H), 3.40 (d, J = 4.6 Hz, 1H), 3.30 (s, 3H), 3.14 (d, J = 9.8 Hz, 1H). Diastereomer 2: ^{1}H NMR (600 MHz, $CDCl_3$) δ: 7.48−7.45 (m, 6H), 7.28−7.23 (m, 6H), 7.21−7.15 (m, 3H), 3.77 (dd, J = 11.1, 2.7 Hz, 1H), 3.72 (s, 3H), 3.59 (d, J = 2.7 Hz, 1H), 3.22 (s, 3H), 2.98 (d, J = 11.0 Hz, 1H). Diastereomer 1: ^{13}C NMR (151 MHz, $CDCl_3$) δ: 173.4, 172.2, 145.8, 128.9, 128.1, 126.7, 71.4, 59.5, 58.4, 52.2, 52.0. Diastereomer 2: ^{13}C NMR (151 MHz, $CDCl_3$) δ: 173.9, 172.9, 145.6, 129.0, 128.0, 126.7, 70.8, 59.3, 58.1, 52.5, 52.1.

In Silico Study. The modeling study was performed using the software package MOE 2015 (Molecular Operating Environment, Chemical Computing Group) using the built-in mmff94x force field and the GB/SA continuum solvation model. Docking: The receptor proteins were prepared for docking by running the algorithm Protonate 3D. Docking studies were performed using the *Rigid Fit* algorithm under standard setup with the mmff94x force field, solvation set to distance, and *ligand atoms* selected as docking site. Homology models: the amino acid sequences of human EAAT1-3 were aligned with that of the bacterial homolog Glt_{Ph} (PDB code: 2nww). After this a small segment present in the EAATs but not in Glt_{Ph} was truncated from the EAAT sequences (see Supporting Information for details). Homology models were build on the 3D coordinates of Glt_{Ph} (PDB code: 2nww) by applying parameters from standard setup (see Supporting Information for details).

Cell Culture and [^{3}H]-D-Aspartate Uptake Assay. All cell culture reagents were from ThermoFisher Scientific (Waltham, MA). Stable EAAT1-, EAAT2-, and EAAT3-HEK293 cell lines established as described previously[14] were maintained in DMEM with high glucose and GlutaMAX supplemented with 5% dialyzed FBS, 100 U/mL penicillin, 100 μg/mL streptomycin, and 1 mg/L G418, and the uptake assay was performed essentially as previously described.[14] Briefly, cells were seeded in 96-well OptiPlates (PerkinElmer, Boston, MA), reaching confluence after 16−24 h, where they were washed in 100 μL of room temperature uptake buffer (Hank's Buffered Saline Solution (ThermoFisher) supplemented with 20 mM HEPES, 1 mM $CaCl_2$, and 1 mM $MgCl_2$ (all from Sigma, St. Louis, MO), pH 7.4). Cells were then incubated for 3 min at room temperature in 50 μL of uptake buffer with 100 nM [^{3}H]-D-aspartate (PerkinElmer) and various concentrations of the test compounds, washed twice in ice-cold uptake buffer before 150 μL of MicroScint20 (PerkinElmer) was added, and the plates were shaken vigorously for ≥1 h before reading in a TopCount NXT (PerkinElmer).

■ ASSOCIATED CONTENT

Supporting Information

The Supporting Information is available free of charge on the ACS Publications website at DOI: 10.1021/acs.jmedchem.6b01066.

Sequence alignment of EAAT1−3 with Glt_{Ph} (PDB code: 2nww) (PDF)

3D coordinates of Figure 4 (PDB format) (PDB)

Molecular formula strings (CSV)

■ AUTHOR INFORMATION

Corresponding Author

*Phone: +45 35 33 62 44. E-mail: lebu@sund.ku.dk.

Notes

The authors declare no competing financial interest.

■ ACKNOWLEDGMENTS

We thank the Danish Medical Research Council, Lundbeck Foundation, the Novo Nordisk Foundation, the Augustinus Foundation, and the Carlsberg Foundation for financial support.

■ ABBREVIATIONS USED

CNS, central nervous system; dr, diastereomeric ratio; EAAT, excitatory amino acid transporter; KHMDS, potassium hexamethyldisilazide; LHMDS, lithium hexamethyldisilazide; TEA, triethylamine; Tr, trityl; TBOA, *threo*-benzyloxy aspartate; EBOA, *erythro*-benzyloxy aspartate; DHK, dihydrokainic acid; DIPEA, diisopropylethyl amine

■ REFERENCES

(1) Moghaddam, B.; Javitt, D. From Revolution to Evolution: The Glutamate Hypothesis of Schizophrenia and Its Implication for Treatment. *Neuropsychopharmacology* **2012**, *37*, 4−15.

(2) Machado-Vieira, R.; Henter, I. D.; Zarate, C. A., Jr. New Targets for Rapid Antidepressant Action. *Prog. Neurobiol.* **2015**, 10.1016/j.pneurobio.2015.12.001.

(3) Gonzalez, J.; Jurado-Coronel, J. C.; Ávila, M. F.; Sabogal, A.; Capani, F.; Barreto, G. E. NMDARs in Neurological Diseases: A Potential Therapeutic Target. *Int. J. Neurosci.* **2015**, *125*, 315−327.

(4) Finlay, C.; Duty, S. Therapeutic Potential of Targeting Glutamate Receptors in Parkinson's Disease. *J. Neural Transm.* **2014**, *121*, 861−880.

(5) Danbolt, N. C. Glutamate Uptake. *Prog. Neurobiol.* **2001**, *65*, 1−105.

(6) Bunch, L.; Erichsen, M. N.; Jensen, A. A. Excitatory Amino Acid Transporters as Potential Drug Targets. *Expert Opin. Ther. Targets* **2009**, *13*, 719−731.

(7) Jiang, J.; Amara, S. G. New Views of Glutamate Transporter Structure and Function: Advances and Challenges. *Neuropharmacology* **2011**, *60*, 172−181.

(8) Vandenberg, R. J.; Ryan, R. M. Mechanisms of Glutamate Transport. *Physiol. Rev.* **2013**, *93*, 1621−1657.

(9) Jensen, A. A.; Fahlke, C.; Bjørn-Yoshimoto, W. E.; Bunch, L. Excitatory amino acid transporters: recent insights into molecular mechanisms, novel modes of modulation and new therapeutic possibilities. *Curr. Opin. Pharmacol.* **2015**, *20*, 116−123.

(10) Grewer, C.; Gameiro, A.; Rauen, T. SLC1 Glutamate Transporters. *Pfluegers Arch.* **2014**, *466*, 3−24.

(11) Traynelis, S. F.; Wollmuth, L. P.; McBain, C. J.; Menniti, F. S.; Vance, K. M.; Ogden, K. K.; Hansen, K. B.; Yuan, H.; Myers, S. J.; Dingledine, R. Glutamate Receptor Ion Channels: Structure, Regulation, and Function. *Pharmacol. Rev.* **2010**, *62*, 405−496.

(12) Shimamoto, K.; Lebrun, B.; Yasuda-Kamatani, Y.; Sakaitani, M.; Shigeri, Y.; Yumoto, N.; Nakajima, T. DL-Threo-Beta-Benzyloxyaspartate, a Potent Blocker of Excitatory Amino Acid Transporters. *Mol. Pharmacol.* **1998**, *53*, 195−201.

(13) Lebrun, B.; Sakaitani, M.; Shimamoto, K.; Yasuda-Kamatani, Y.; Nakajima, T. New β-Hydroxyaspartate Derivatives Are Competitive

DOI: 10.1021/acs.jmedchem.6b01066
J. Med. Chem. XXXX, XXX, XXX−XXX

Blockers for the Bovine Glutamate/Aspartate Transporter. *J. Biol. Chem.* **1997**, *272*, 20336−20339.
(14) Jensen, A. A.; Bräuner-Osborne, H. Pharmacological Characterization of Human Excitatory Amino Acid Transporters EAAT1, EAAT2 and EAAT3 in a Fluorescence-Based Membrane Potential Assay. *Biochem. Pharmacol.* **2004**, *67*, 2115−2127.
(15) Arriza, J.; Fairman, W.; Wadiche, J.; Murdoch, G.; Kavanaugh, M.; Amara, S. Functional Comparisons of Three Glutamate Transporter Subtypes Cloned from Human Motor Cortex. *J. Neurosci.* **1994**, *14*, 5559−5569.
(16) Sagot, E.; Jensen, A. A.; Pickering, D. S.; Pu, X.; Umberti, M.; Stensbøl, T. B.; Nielsen, B.; Assaf, Z.; Aboab, B.; Bolte, J.; Gefflaut, T.; Bunch, L. Chemo-Enzymatic Synthesis of (2S,4R)-2-Amino-4-(3-(2,2-Diphenylethylamino)-3-Oxopropyl)pentanedioic Acid: A Novel Selective Inhibitor of Human Excitatory Amino Acid Transporter Subtype 2. *J. Med. Chem.* **2008**, *51*, 4085−4092.
(17) Dunlop, J.; McIlvain, H. B.; Carrick, T. A.; Jow, B.; Lu, Q.; Kowal, D.; Lin, S.; Greenfield, A.; Grosanu, C.; Fan, K.; Petroski, R.; Williams, J.; Foster, A.; Butera, J. Characterization of Novel Aryl-Ether, Biaryl, and Fluorene Aspartic Acid and Diaminopropionic Acid Analogs as Potent Inhibitors of the High-Affinity Glutamate Transporter EAAT2. *Mol. Pharmacol.* **2005**, *68*, 974−982.
(18) Vandenberg, R. J.; Mitrovic, A. D.; Chebib, M.; Balcar, V. J.; Johnston, G. A. R. Contrasting Modes of Action of Methylglutamate Derivatives on the Excitatory Amino Acid Transporters, EAAT1 and EAAT2. *Mol. Pharmacol.* **1997**, *51*, 809−815.
(19) Alaux, S.; Kusk, M.; Sagot, E.; Bolte, J.; Jensen, A. a; Bräuner-Osborne, H.; Gefflaut, T.; Bunch, L. Chemoenzymatic Synthesis of a Series of 4-Substituted Glutamate Analogues and Pharmacological Characterization at Human Glutamate Transporters Subtypes 1−3. *J. Med. Chem.* **2005**, *48*, 7980−7992.
(20) Abrahamsen, B.; Schneider, N.; Erichsen, M. N.; Huynh, T. H.; Fahlke, C.; Bunch, L.; Jensen, A. A. Allosteric Modulation of an Excitatory Amino Acid Transporter: The Subtype-Selective Inhibitor UCPH-101 Exerts Sustained Inhibition of EAAT1 through an Intramonomeric Site in the Trimerization Domain. *J. Neurosci.* **2013**, *33*, 1068−1087.
(21) Jensen, A. A.; Erichsen, M. N.; Nielsen, C. W.; Stensbøl, T. B.; Kehler, J.; Bunch, L. Discovery of the First Selective Inhibitor of Excitatory Amino Acid Transporter Subtype 1. *J. Med. Chem.* **2009**, *52*, 912−915.
(22) Erichsen, M. N.; Huynh, T. H. V.; Abrahamsen, B.; Bastlund, J. F.; Bundgaard, C.; Monrad, O.; Bekker-Jensen, A.; Nielsen, C. W.; Frydenvang, K.; Jensen, A. A.; Bunch, L. Structure−Activity Relationship Study of First Selective Inhibitor of Excitatory Amino Acid Transporter Subtype 1:2-Amino-4-(4-Methoxyphenyl)-7-(Naphthalen-1-Yl)-5-Oxo-5,6,7,8-Tetrahydro-4 H -Chromene-3-Carbonitrile (UCPH-101). *J. Med. Chem.* **2010**, *53*, 7180−7191.
(23) Haym, I.; Huynh, T. H. V; Hansen, S. W.; Pedersen, M. H. F.; Ruiz, J. A.; Erichsen, M. N.; Gynther, M.; Bjørn-Yoshimoto, W. E.; Abrahamsen, B.; Bastlund, J. F.; Bundgaard, C.; Eriksen, A. L.; Jensen, A. A.; Bunch, L. Bioavailability Studies and in Vitro Profiling of the Selective Excitatory Amino Acid Transporter Subtype 1 (EAAT1) Inhibitor UCPH-102. *ChemMedChem* **2016**, *11*, 403−419.
(24) Hansen, S. W.; Erichsen, M. N.; Fu, B.; Bjørn-Yoshimoto, W. E.; Abrahamsen, B.; Hansen, J. C.; Jensen, A. A.; Bunch, L. Identification of a New Class of Selective Excitatory Amino Acid Transporter Subtype 1 (EAAT1) Inhibitors Followed by a Structure−Activity Relationship Study. *J. Med. Chem.* **2016**, *59*, 10.1021/acs.jmedchem.6b01058.
(25) Esslinger, C. S.; Agarwal, S.; Gerdes, J.; Wilson, P. A.; Davis, E. S.; Awes, A. N.; O'Brien, E.; Mavencamp, T.; Koch, H. P.; Poulsen, D. J.; Rhoderick, J. F.; Chamberlin, A. R.; Kavanaugh, M. P.; Bridges, R. J. The Substituted Aspartate Analogue L-Beta-Threo-Benzyl-Aspartate Preferentially Inhibits the Neuronal Excitatory Amino Acid Transporter EAAT3. *Neuropharmacology* **2005**, *49*, 850−861.
(26) Bunch, L.; Nielsen, B.; Jensen, A. a; Bräuner-Osborne, H. Rational Design and Enantioselective Synthesis of (1R,4S,5R,6S)-3-azabicyclo[3.3.0]octane-4,6-Dicarboxylic Acid - a Novel Inhibitor at Human Glutamate Transporter Subtypes 1, 2, and 3. *J. Med. Chem.* **2006**, *49*, 172−178.
(27) Kanai, Y.; Hediger, M. A. Primary Structure and Functional Characterization of a High-Affinity Glutamate Transporter. *Nature* **1992**, *360*, 467−471.
(28) Leuenberger, M.; Ritler, A.; Simonin, A.; Hediger, M. A.; Lochner, M. Concise Asymmetric Synthesis and Pharmacological Characterization of All Stereoisomers of Glutamate Transporter Inhibitor TFB-TBOA and Synthesis of EAAT Photoaffinity Probes. *ACS Chem. Neurosci.* **2016**, *7*, 534−539.
(29) Shimamoto, K.; Sakai, R.; Takaoka, K.; Yumoto, N.; Nakajima, T.; Amara, S. G.; Shigeri, Y. Characterization of Novel L-Threo-Benzyloxyaspartate Derivatives, Potent Blockers of the Glutamate Transporters. *Mol. Pharmacol.* **2004**, *65*, 1008−1015.
(30) Shimamoto, K.; Shigeri, Y.; Yasuda-Kamatani, Y.; Lebrun, B.; Yumoto, N.; Nakajima, T. Syntheses of Optically Pure β-Hydroxyaspartate Derivatives as Glutamate Transporter Blockers. *Bioorg. Med. Chem. Lett.* **2000**, *10*, 2407−2410.
(31) Mavencamp, T. L.; Rhoderick, J. F.; Bridges, R. J.; Esslinger, C. S. Synthesis and Preliminary Pharmacological Evaluation of Novel Derivatives of L-β-Threo-Benzylaspartate as Inhibitors of the Neuronal Glutamate Transporter EAAT3. *Bioorg. Med. Chem.* **2008**, *16*, 7740−7748.
(32) Meadows, E. S.; De Wall, S. L.; Barbour, L. J.; Gokel, G. W. Alkali Metal Cation - π Interactions Observed by Using a Lariat Ether Model System. *J. Am. Chem. Soc.* **2001**, *123*, 3092−3107.
(33) Zhong, W.; Gallivan, J. P.; Zhang, Y.; Li, L.; Lester, H. A.; Dougherty, D. A. From Ab Initio Quantum Mechanics to Molecular Neurobiology: A Cation-Pi Binding Site in the Nicotinic Receptor. *Proc. Natl. Acad. Sci. U. S. A.* **1998**, *95*, 12088−12093.
(34) True, J. E.; Thomas, T. D.; Winter, R. W.; Gard, G. L. Electronegativities from Core-Ionization Energies: Electronegativities of SF5 and CF3. *Inorg. Chem.* **2003**, *42*, 4437−4441.
(35) Assaf, Z.; Larsen, A. P.; Venskutonytė, R.; Han, L.; Abrahamsen, B.; Nielsen, B.; Gajhede, M.; Kastrup, J. S.; Jensen, A. a; Pickering, D. S.; Frydenvang, K.; Gefflaut, T.; Bunch, L. Chemoenzymatic Synthesis of New 2,4-Syn-Functionalized (S)-Glutamate Analogues and Structure-Activity Relationship Studies at Ionotropic Glutamate Receptors and Excitatory Amino Acid Transporters. *J. Med. Chem.* **2013**, *56*, 1614−1628.
(36) Boudker, O.; Ryan, R. M.; Yernool, D.; Shimamoto, K.; Gouaux, E. Coupling Substrate and Ion Binding to Extracellular Gate of a Sodium-Dependent Aspartate Transporter. *Nature* **2007**, *445*, 387−393.

DOI: 10.1021/acs.jmedchem.6b01066
J. Med. Chem. XXXX, XXX, XXX−XXX